24. Sekiya, S., Yamaguchi, Y., Kato, K., and Tanaka, K. (2005) Mechanistic elucidation of formation of reduced 2-aminopyridine-derivatized oligosaccharide and their application in matrix assisted desorption/ionization mass spectrometry. *Rapid Commun. Mass Spectrom.* **19**, 3607–3611

25. Shirato, H., Ogawa, S., Ito, H., Sato, T., Kameyama, A., Narimatsu, H., Zheng, X., Miyamura, T., Wakita, T., Ishii, K., and Takeda, N. (2008) Noroviruses distinguish between Type 1 and Type 2 histo-blood group antigens for binding. *J. Virol.* **82**, 10756–10767

Development 136, 2511-2521 (2009) doi:10.1242/dev.037168

Two distinct types of mouse melanocyte: differential signaling requirement for the maintenance of non-cutaneous and dermal versus epidermal melanocytes

Hitomi Aoki[1], Yasuhiro Yamada[2], Akira Hara[2] and Takahiro Kunisada[1,*]

Unlike the thoroughly investigated melanocyte population in the hair follicle of the epidermis, the growth and differentiation requirements of the melanocytes in the eye, harderian gland and inner ear – the so-called non-cutaneous melanocytes – remain unclear. In this study, we investigated the in vitro and in vivo effects of the factors that regulate melanocyte development on the stem cells or the precursors of these non-cutaneous melanocytes. In general, a reduction in KIT receptor tyrosine kinase signaling leads to disordered melanocyte development. However, melanocytes in the eye, ear and harderian gland were revealed to be less sensitive to KIT signaling than cutaneous melanocytes. Instead, melanocytes in the eye and harderian gland were stimulated more effectively by endothelin 3 (ET3) or hepatocyte growth factor (HGF) signals than by KIT signaling, and the precursors of these melanocytes expressed the lowest amount of KIT. The growth and differentiation of these non-cutaneous melanocytes were specifically inhibited by antagonists for ET3 and HGF. In transgenic mice induced to express ET3 or HGF in their skin and epithelial tissues from human cytokeratin 14 promoters, the survival and differentiation of non-cutaneous and dermal melanocytes, but not epidermal melanocytes, were enhanced, apparently irrespective of KIT signaling. These results provide a molecular basis for the clear discrimination between non-cutaneous or dermal melanocytes and epidermal melanocytes, a difference that might be important in the pathogenesis of melanocyte-related diseases and melanomas.

KEY WORDS: Melanocytes, c-KIT, KITL, Endothelin, HGF, Mouse

INTRODUCTION

Melanocytes develop from the pluripotent neural crest, which also gives rise to a number of other cell types, including neurons and glial cells of the peripheral nervous system as well as bone and cartilage cells of the head skeleton. Their immature form, called the melanoblast, migrates along characteristic pathways to various destinations, such as the dermis and epidermis, the inner ear and the choroids of the eye (for reviews, see Hall, 1999; Le Douarin and Kalcheim, 1999).

The proliferation and differentiation of melanocytes in hair follicles are closely coupled with the hair regeneration cycle. The follicular melanocytes comprise a stem cell system, and melanocyte stem cells reside in the upper permanent portion of the hair follicles throughout the hair cycle (Nishimura et al., 2002). The eye, harderian gland and ear are also abundant in melanocytes; however, unlike in the hair follicles, no obvious spatially restricted niche of melanocyte stem cells has been described in these organs (Boissy, 1999).

Numerous signaling systems and transcription factors regulate all aspects of melanocyte development. These include the Wnt signaling pathway (Ikeya et al., 1997; Dorsky et al., 2000); the G-coupled endothelin B receptor (EDNRB) and its ligand, endothelin 3 (ET3; EDN3) (Baynash et al., 1994; Hosoda et al., 1994; Pavan and Tilghman, 1994); the tyrosine kinase receptor KIT and its ligand, KITL [also known as stem cell factor (SCF) or mast cell growth factor (MGF)] (Geissler et al., 1988; Cable et al., 1995; Wehrle-Haller and Weston, 1995); the hepatocyte growth factor (HGF) and its ligand, c-MET (McGill et al., 2006; Kos et al., 1999); and the transcription factors PAX3 (Watanabe et al., 1998; Potterf et al., 2000), SOX10 (Pingault et al., 1998; Southard-Smith et al., 1998; Potterf et al., 2000) and MITF, which is a basic helix-loop-helix leucine-zipper protein (Hodgkinson et al., 1993; Opdecamp et al., 1997; Nakayama et al., 1998; Lister et al., 1999). More recently, it was reported that PTEN (Inoue-Narita et al., 2008; Sarin and Artandi, 2007), Notch (Moriyama et al., 2006; Aubin-Houzelstein et al., 2008; Osawa and Fisher, 2008), FGF2 (Weiner at al., 2007; Barsh and Cotsarelis, 2007; Yonetani et al., 2008) and BCL2 (Mak et al., 2006; Nishimura et al., 2005; McGill et al., 2002) are also involved in melanocyte development. Among the genes that encode these factors, the extensively studied signaling ligand and receptor pairs, *Kitl-Kit* and *Et3-Ednrb*, provide a particularly intriguing set, as mutations in any one of them leads to a strikingly overlapping phenotype. Thus, mice with such mutations are viable but show the early loss of cells of the melanocyte lineage, which leads to white spotting phenotypes and, sometimes, to a predominately white coat color (Baynash et al., 1994; Hosoda et al., 1994; Yoshida et al., 2001; Botchkareva et al., 2001).

Using cultures of embryonic stem (ES) cells for the induction of melanocyte differentiation in vitro, we previously investigated the requirement for EDNRB signaling throughout the entire process of melanocyte development, in association with that for KIT signaling (Aoki et al., 2005). *Kit* homozygous knockout ($Kit^{W\text{-}lacZ}/Kit^{W\text{-}lacZ}$) ES cells, which were completely defective for melanocyte development, were significantly and dose dependently compensated by the addition of ET3 in vitro, and forced expression of ET3 in the skin reduced the white spot area of Kit^{W57}/Kit^{W57} mice in vivo (Aoki et al., 2005). Although KIT and EDNRB signaling are individually indispensable for the survival and maintenance of melanocyte lineage cells, at least during a certain period of development (Yoshida et al., 1996a; Shin et al., 1999), these two signals are thought to influence each other.

[1]Department of Tissue and Organ Development, Regeneration, and Advanced Medical Science, Gifu University Graduate School of Medicine, 1-1, Yanagido, Gifu 501-1194, Japan. [2]Department of Tumor Pathology, Gifu University Graduate School of Medicine, 1-1, Yanagido, Gifu 501-1194, Japan.

*Author for correspondence (e-mail: tkunisad@gifu-u.ac.jp)

Accepted 21 May 2009

It is very typical of transgenic mice in which KITL expression in the skin is induced by the cytokeratin 14 promoter that melanocyte development in specific areas of the skin is extremely progressive, and in such mice, the nose and foot-pad regions are filled with fully pigmented melanocytes as early as the newborn stage (Kunisada et al., 1998). The molecular basis for these observations is still not clear, but it appears that the environment is not uniformly favorable for melanocyte development even under the controlled expression of a single influential factor. Instead, melanocytes may react differentially to the signal in a spatially distinctive manner and region-specific melanocyte cell types might exist.

In the present study, we compared the dependencies of non-cutaneous and cutaneous (epidermal and dermal) melanocytes on KIT, EDNRB, HGF and other signals, using various genetic and cytological approaches. The results suggested that the non-cutaneous and dermal melanocytes were not as sensitive to KIT signaling as the epidermal melanocytes and instead depended more on ET3 and HGF signaling than KIT signaling. As for the cutaneous melanocytes, experimentally induced dermal melanocytes behaved more similarly to those of non-cutaneous tissues. In the light of these findings, we propose the existence of two major melanocyte populations: KIT-sensitive cutaneous melanocytes in the epidermis and weakly KIT-sensitive non-cutaneous and dermal melanocytes. Our classification, based on the growth requirements of the melanocytes, might provide new insight into the characterization of melanocytes in various animals and into the origins of human melanocyte-related diseases.

MATERIALS AND METHODS

Animals

All animal experiments were approved by the Animal Research Committee of the Graduate School of Medicine, Gifu University. ICR mice, C57BL/6 mice and *W/W*^{v} mice were obtained from Japan SLC (Shizuoka, Japan). The following transgenic mice were maintained in our animal facility: those generated with the human cytokeratin 14 promoter (hk14) driving cytokine/growth factor cDNAs [hk14-ET3 (Yamazaki et al., 2005); hk14-KITL (Kunisada et al., 1998); hk14-HGF (Kunisada et al., 2000)]; Kit Val620Ala transgenic mice (Tosaki et al., 2006); *W*^{v}/*W*^{v} and *W/W* mice derived from *W*^{v}/+ and *W*/+ mice; DCT-lacZ transgenic mice (Mackenzie et al., 1997); and C57Bl/6 background CAG-EGFP mice (RIKEN, BRC). CAG-CAT-EGFP mice (a gift from J. Miyazaki, Osaka University, Osaka, Japan) (Kawamoto et al., 2000) were bred with *Dct*$^{tm1(Cre)Bee}$ mice (a gift from F. Beermann, Swiss Institute for Experimental Cancer Research, Epalinges, Switzerland) to generate compound heterozygotes (Yonetani et al., 2008; Osawa et al., 2005). Genotyping was performed as described previously (Guyonneau et al., 2004).

Mice were housed in standard animal rooms with food and water ad libitum under controlled humidity and temperature (22±2°C) conditions. The room was illuminated by fluorescent lights that were on from 8:00 to 20:00 hours.

Cell preparation

Postnatal day (P) 0 or P3 mice were sacrificed by decapitation and ear capsules, nose, eyes, harderian glands and skin were quickly dissected on ice. The ear capsules were dissected into very small pieces. The nasal vibrissae were collected from the opposite side of the epidermis (vibrissae hair follicle) one by one, and dissected into very small fragments. The eyes were separated into cornea, lens, and neural retina; each was dissected into very small pieces (Aoki et al., 2008a). The harderian glands were also dissected into very small fragments. These small pieces of all these tissues were treated for 30 minutes at 37°C or overnight at 4°C with 0.25% trypsin/1 mM EDTA (Invitrogen, USA), 0.1% collagenase I (Sigma-Aldrich, USA) and 1× dispase (Roche, Switzerland). The skin was treated with 0.25% trypsin/1 mM EDTA for 30 minutes at 37°C or overnight at 4°C. Then, the epidermis was peeled off the underlying dermis and each layer collected separately and dissected into very small pieces. The cells of these small pieces were dissociated by gentle pipetting, and the cell suspensions strained through 400-mesh nylon (Sansho, Japan).

Cell culture

Ten thousand cells prepared from each tissue as described above were inoculated into 6-well plates previously seeded with ST2 cells or into gelatin-coated plates and cultured in Alpha Minimum Essential Medium (Invitrogen) supplemented with 10% fetal calf serum (FCS) (Equitech-Bio, USA or Nichirei Bioscience, Japan). They were maintained under 5% CO_2 at 37°C. Then, 40 pM basic fibroblast growth factor (bFGF; FGF2) (R&D Systems, USA), 10 nM dexamethasone (Dex) (Sigma) and 10 pM cholera toxin (CT) (Sigma) were added and remained present during the culture period. The medium was changed every 3 days (Aoki et al., 2008b).

The specific inhibitors and corresponding concentrations used for cell culture were: 10 μg/ml ACK2, which is a neutralizing antibody for KIT (see final section of Materials and methods); 100 ng/ml BQ788, which inhibits EDNRB (Peptides International, USA); 5 μM γ-secretase inhibitor, which is used as a Notch inhibitor; 25 μM PD98059, a MEK kinase inhibitor; 5 μM MET kinase inhibitor, used as an HGF inhibitor; 10 μM SU1498, a VEGFR inhibitor; 10 μM SU5402, an FGFR inhibitor; 10 μM AG1433, an EGFR inhibitor; and 5 μM SB203580, a p38 inhibitor (all from Merck, Germany).

Flow cytometric analysis and cell sorting

Cell suspensions of ear capsules, vibrissae, choroid, harderian glands, epidermis and dermis prepared from P0 DCT-lacZ mice or P3 *Dct*$^{tm1(Cre)Bee}$/CAG-CAT-EGFP mice as described above were centrifuged and resuspended in staining medium [SM, PBS containing 3% fetal calf serum (FCS)]. The dissociated cells were then blocked with rat anti-mouse Fc gamma receptor (2.4-G2, BD Bioscience) on ice for 30-40 minutes. After another wash with SM, the cells were stained with phycoerythrin (PE)-conjugated rat anti-mouse CD45 (PTPRC) (30-F11, BD Bioscience) on ice for 30-40 minutes, washed, and incubated with allophycocyanin (APC)-conjugated rat anti-mouse c-KIT (2B8, BD Bioscience) on ice for 30-40 minutes. The cells were washed and resuspended in SM containing 3 mg/ml propidium iodide (PI) (Calbiochem, USA). All cell sorting and analyses were performed with a FACS Aria dual-laser flow cytometer (BD Bioscience). The sorted cells were directly inoculated into 6-well plates previously seeded with ST2 stromal cells using the ACDU System (BD Bioscience).

Histology

Mice were killed with an overdose of sodium pentobarbital (200 mg/kg). The eyes were enucleated and fixed by immersion overnight in 10% formalin in phosphate buffer (pH 7.2). The methods used for histological analysis have been described in detail previously (Aoki et al., 2008c). Briefly, eyes were dehydrated with ethanol, soaked in xylene and embedded in paraffin. Horizontal serial sections were prepared at 3 μm and stained with Hematoxylin and Eosin (HE).

lacZ staining

lacZ staining was performed as reported in detail previously (Yoshida et al., 1996b). In brief, cells were fixed for 10 minutes in 2% paraformaldehyde supplemented with 0.2% glutaraldehyde and 0.02% Tween 20. After three washes in PBS, the cells were stained overnight at 37°C in 10 mM phosphate buffer (pH 7.2) containing 1.0 mM $MgCl_2$, 3.1 mM $K_4[Fe(CN)_6]$, 3.1 mM $K_3[Fe(CN)_6]$ and 2 mg/ml X-Gal. The staining reaction was stopped by washing in PBS. The specimens were post-fixed overnight in 10% formalin in phosphate buffer (pH 7.2).

Production and microinjection of monoclonal antibody

The rat monoclonal antibody ACK2 against the c-KIT receptor protein, which can block c-KIT function, and its class-matched control monoclonal antibody were described previously (Nishikawa et al., 1991).

The ACK2 antibody was microinjected into each fetal amniotic cavity at embryonic day (E) 11-12.5 as previously described (Yoshida et al., 1993). In brief, 1 μl of antibody solution (0.2-40 mg/ml) was injected into each amniotic cavity of pregnant females with a glass micropipette of ~50-70 μm diameter. The pipette was manually inserted anywhere in the

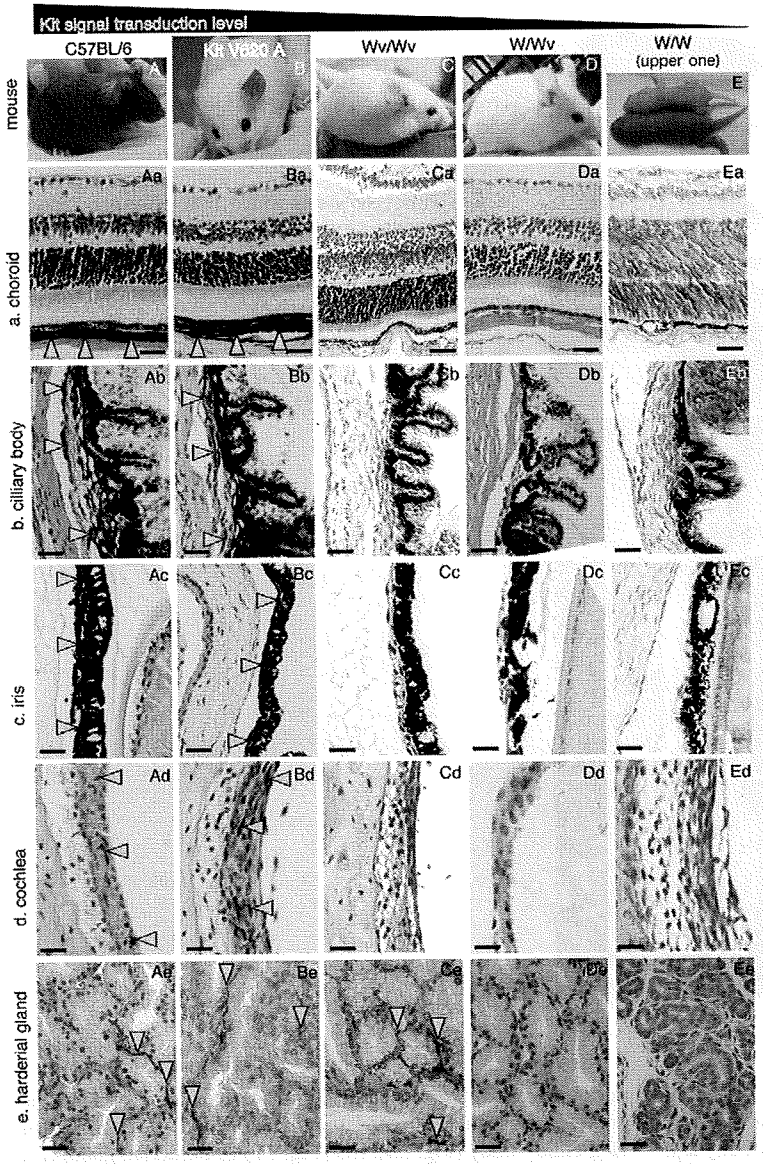

Fig. 1. Differential KIT signaling and melanocyte distribution in *Kit* mutant transgenic mice. **(A-Ee)** C57BL/6 (A), Kit V620A (B), W^v/W^v (C), W/W^v (D) and W/W (pink pup at top of E, with wild-type littermate pup beneath it) mice, arranged from left to right according to the decrease in the KIT signal level. Melanocyte localization is shown in the uvea, including the choroid (Aa-Ea), ciliary body (Ab-Eb) and iris (Ac-Ec), and in the cochlea (Ad-Ed) and harderian gland (Ae-Ee). For example, melanocytes exist not only in hair follicles, but also in the uvea including the choroid (Aa), ciliary body (Ab) and iris (Ac), as well as in the cochlea (Ad) and harderian gland (Ae), in C57Bl/6 control mice. By contrast, W/W^v (D) and W/W (E) mice had no melanocytes in their hair follicles or in any of the regions mentioned above. In W^v/W^v (C) and Kit V620A (B) mice, no melanocytes were found in the hair follicles, except in the ears. Kit V620A mice often had pigmented ears (B), and most of the non-cutaneous melanocytes in their eyes, such as those in the choroid (Ba), ciliary body (Bb), and iris (Bc), as well as melanocytes in the cochlea (Bd) and harderian gland (Be), developed normally. In W^v/W^v mice, melanocytes were detected in the harderian gland. Arrowheads indicate the melanocytes. Scale bars: 25 μm, except 50 μm in Aa-Ea.

antimesometrial third of the embryo beneath the placenta. Some of the fetuses that received a high concentration of ACK2 (e.g. over 15-20 mg/ml) died as embryos or around birth. Some surviving littermates treated with this procedure were maintained for more than 1.5 years to observe the long-term effect of the antibody treatment on coat color spotting patterns, the stability of the pattern with age and fertility, and to monitor for any behavioral abnormalities.

RESULTS

Distribution of non-cutaneous melanocytes in *Kit* coat color mutants

A mouse model of human piebaldism comprising the Val620Ala mutation in the *Kit* gene shows various coat-pigmentation patterns among the transgenic lines generated ($Kit^{V620A}Tg$–1 and $Kit^{V620A}Tg$–4) (Tosaki et al., 2006). Occasionally, phenotypes varied within the same transgenic line. For example, in $Kit^{V620A}Tg$–4, which is a relatively less pigmented line, we sometimes found almost completely white individuals (Fig. 1B). Spontaneous *Kit* mutants, such as $W/+$ and $W^v/+$, also had white spots, and homozygous W/W, W^v/W^v or W/W^v mice showed a completely white coat color (Fig. 1C-E).

For these mice, which exhibit different KIT signal transduction levels, we investigated the localization of melanocytes, especially those in the non-cutaneous tissues such as the uvea (i.e. the choroid, ciliary body and iris), the cochlea and the harderian gland. C57BL/6 and $Kit^{V620A}Tg$, W^v/W^v, W/W^v and W/W mutant mice are arranged in Fig. 1 from left to right in accordance with the expected KIT signal transduction level, under which are shown histological representations of melanocytes in their choroid, ciliary body, iris, cochlea and harderian gland. Melanocytes were present in all these tissues of C57BL/6 control mice (Fig. 1Aa-e), whereas no melanocytes were found in the same tissues from W/W^v or W/W mice (Fig. 1Da-e,Ea-e). In $Kit^{V620A}Tg$ mice, although they had no melanocytes in their hair follicles, melanocytes were detected in the ear capsules, and the melanocytes in their eyes (choroid, ciliary body, iris and harderian gland), as well as those in the cochlea in the

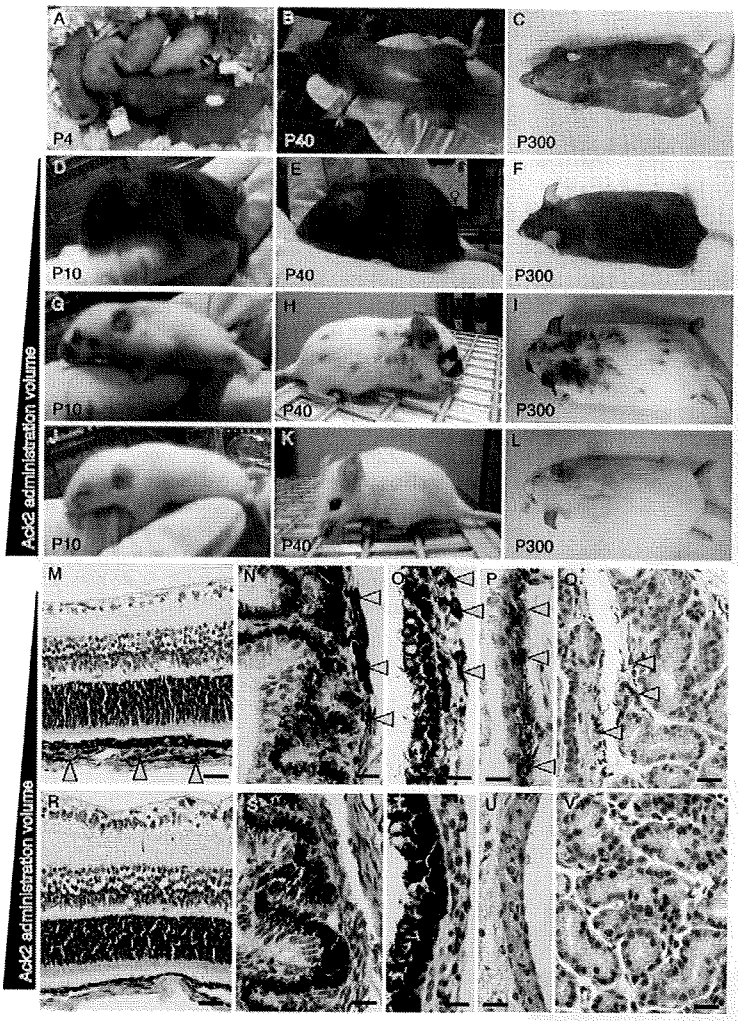

Fig. 2. KIT signal blockade with various doses of ACK2 and effects on melanocyte development. (**A-L**) Mice administered ACK2 on E12 were observed at P4, P10, P40 and P300 as labeled. (**M-V**) Hematoxylin and Eosin (HE) staining of choroid (M,R), cillia (N,S), iris (O,T), cochlea (P,U) and harderian gland (Q,V). Arrowheads indicate the melanocytes. Administration of the KIT antagonistic antibody ACK2 (20 μg) into E12 C57BL/6 mouse fetuses eliminated whole melanocyte populations including non-cutaneous melanocytes (J-L,R-V). A reduced amount of ACK2 (0.5-10 μg) allowed the differentiation of non-cutaneous melanocytes, whereas differentiation of epidermal skin melanocytes was mostly blocked (G-I,M-Q). A control mouse, which was administered with very little ACK2 (D-F), often had a small white spot only on its belly (B,C). Scale bars: 25 μm, except 50 μm in M,R.

inner ear, were found to be distributed normally (Fig. 1Ba-e). In W^v/W^v mice, which also had no melanocytes in their hair follicles, there were no melanocytes in their eyes (choroid, ciliary body and iris) or in their cochlea (Fig. 1Ca-d); however, melanocytes were distributed normally in their ear capsules and harderian gland (Fig. 1Ce). Based on these observations, we hypothesize that these non-cutaneous melanocytes might be less dependent on KIT signaling than the follicular melanocytes, although extensive loss of KIT signals does lead to a complete lack of these non-cutaneous melanocytes.

Development of non-cutaneous melanocytes after temporary inhibition of KIT signaling

To estimate the requirements for KIT signaling in the non-cutaneous mealnocytes, we utilized a neutralizing antibody for the KIT receptor, ACK2, to temporarily inhibit the KIT signaling (Nishikawa et al., 1991). C57BL/6 mice injected with ACK2 (0.2-40 μg) at E11.5-12 lost melanocyte stem cells either partially or completely, a loss that was proportional to the amount of ACK2 injected, as judged by the area of the white spots (Fig. 2; see also Materials and methods). The pigment patterns of these mice remained unchanged throughtout their life (Fig. 2A-L). Among these, completely white mice injected with more than 15 μg of ACK2 had no melanocytes in their ear capsule (Fig. 2J-L), inner ear (Fig. 2U), choroid (Fig. 2R), ciliary body (Fig. 2S), iris (Fig. 2T) or harderian gland (Fig. 2V), whereas the partially pigmented mice injected with 0.5-10 μg of ACK2 had melanocytes in theses areas (Fig. 2G-I,M-Q, arrowheads), in almost the abundance seen in the control C57BL/6 mice (Fig. 1A). These data further support the notion that non-cutaneous melanocytes are less dependent than epidermal melanocytes on KIT signaling during development.

Differential reaction of non-cutaneous melanocytes to ET3 and HGF signaling

Our previous study using transgenic mice generated with *Kitl*, *Et3* or *Hgf* cDNAs driven by the human cytokeratin 14 (*KRT14*) promoter (denoted hk14) indicated that the expression of KITL in the skin induced epidermal skin melanocytosis (Fig. 3C,G,K) and that the expression of ET3 or HGF induced dermal skin melanocytosis (Kunisada et al., 1998; Yamazaki et al., 2005; Kunisada et al., 2000) (Fig. 3A,B,E,F,I,J). Therefore, we determined the effect of the overexpression of these factors on the non-cutaneous melanocytes in the harderian glands of these transgenic mice.

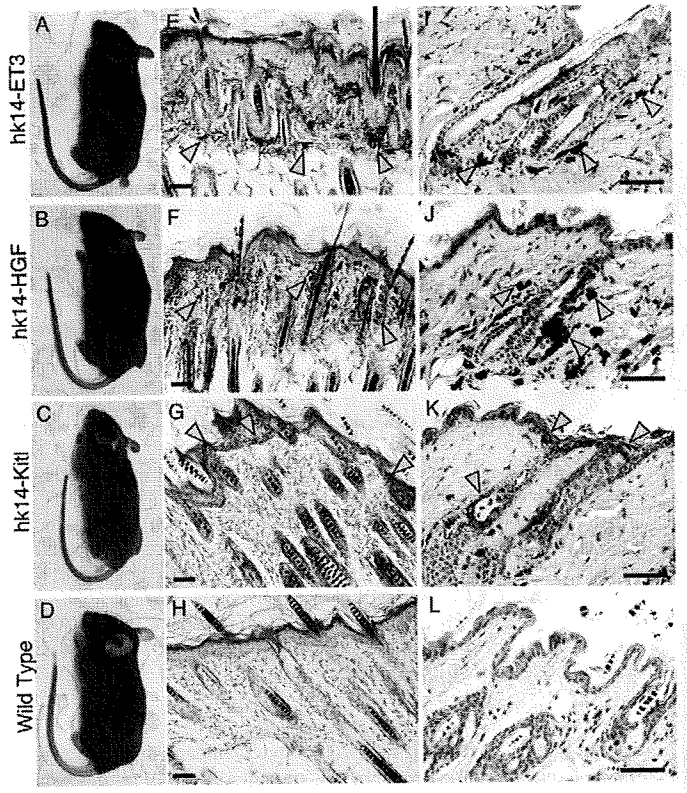

Fig. 3. Melanocyte localization in cutaneous tissue in hk14-HGF, hk14-ET3 and hk14-KITL transgenic mice. (**A-D**) hk14-ET3 (A), hk14-HGF (B) and hk14-KITL (C) transgenic mice and C57Bl/6 wild-type control (D). (**E-L**) Skin sections from hk14-ET3 (E,I), hk14-HGF (F,J) and hk14-KITL (G,K) transgenic mice, and from C57Bl/6 wild-type control (H,L). (I-L) High-magnification views (of different sections from those shown in E-H). Arrowheads indicate pigmented melanocytes sustained in the dermis (E,F,I,J) and epidermis (G,K) of adult mouse skin. Scale bars: 50 μm.

Overall, the melanocytes in the harderian glands were increased in number in these transgenic mice (Fig. 4). In hk14-ET3 mice, the number of melanocytes in the harderian gland was increased (Fig. 4A,E,I), and a significant increase was also observed in hk14-HGF mice (Fig. 4B,F,J), whereas only a slight increase was observed in hk14-KITL mice (Fig. 4C,G,K,Q). In vitro colony formation from the dissociated cells from the dissected harderian gland tissues also revealed that the number of colonies formed was dramatically increased in hk14-ET3 and hk14-HGF mice (Fig. 4M,N), with only a slight increase in hk14-KITL mice (Fig. 4O,R), as compared with the control (Fig. 4P).

In the ocular tissues, the cornea is usually clear, and we observed no melanocytes in the control C57BL6 mice (n=20/20). However, in hk14-ET3 mice we found that dendritic melanocytes had migrated into the cornea (n=20/20; Fig. 5A,D,G,J). Also, pigmented melanocytes, which were not dendritic in shape, were detected in hk14-HGF mice (n=18/20; Fig. 5B,E,H,K). In hk14-KITL mice, we never observed melanocytes in the cornea (n=20/20; Fig. 5C,F,I,L). These observations indicate that transgenically supplied KITL is less effective for the development of non-cutaneous melanocytes of the ocular tissues or harderian gland than ET3 or HGF supplied in the same manner.

Reduced expression of KIT in the non-cutaneous melanocyte precursors and their reduced response to KIT signaling compared with the cutaneous melanocyte precursors

To investigate the molecular basis of the relative ineffectiveness of KITL in the development of non-cutaneous melanocytes, we analyzed KIT expression in the cutaneous and non-cutaneous melanocytes. We previously reported that $KIT^+/CD45^-$ cells in the neonatal skin comprised the developing melanoblast population (Kunisada et al., 1996; Motohashi et al., 2007). In the cutaneous tissues, such as the epidermis, dermis, ear capsule and vibrissa, $KIT^+/CD45^-$ populations were clearly detected by flow cytometry (Fig. 6A-E). However, fewer $KIT^+/CD45^-$ cells were observed in non-cutaneous tissues, such as the uvea in the eye and harderian gland, and the average fluorescence intensity, which indicates the amount of KIT expressed on the cell surface, was clearly reduced in these tissues (Fig. 6F,G). This finding suggests that the lower expression of KIT in the melanocytes of these non-cutaneous tissues is responsible for their lower dependence on KIT signaling.

To further test the differentiation of non-cutaneous melanocytes with respect to KIT expression, we purified 1000 $KIT^+/CD45^-$ cells from P0 DCT-lacZ mice (Mackenzie et al., 1997) and cultured them on ST2 cells (Yamane et al., 1999). After 14 days, pigmented melanocytes and DCT-lacZ-positive melanoblasts were detected among the $KIT^+/CD45^-$ precursors isolated from cutaneous tissues such as the epidermis, dermis, vibrissa and ear capsule, whereas only a few pigmented melanocytes and DCT-lacZ-positive melanoblasts were generated from non-cutaneous tissues such as the uvea and harderian gland (Fig. 7A,B). Most of the colonies generated contained *lacZ*-positive cells, thus confirming the melanocyte cell lineage (Fig. 7B). Thus, very few melanocyte precursors were present in KIT^+ populations in the non-cutaneous tissues.

As we observed a number of non-pigmented but *lacZ*-positive melanoblasts in the neonatal harderian gland of DCT-lacZ mice (see Fig. S1A in the supplementary material), we dissected small pieces of harderian gland from P0 mice and cultured them without stromal cells. Successive observations every other day revealed an increase in the number of pigmented melanocytes by this culture method (see Fig. S1B in the supplementary material). Observation every 12

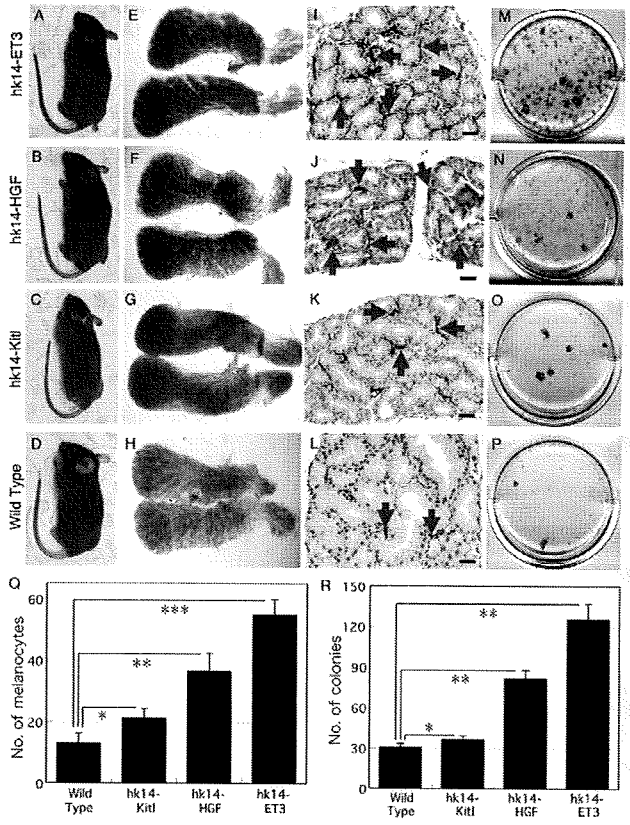

Fig. 4. Effect of exogenous ET3, HGF and KITL expression on melanocyte development in the harderian gland. (**A-P**) hk14-ET3 (A,E,I,M), hk14-HGF (B,F,J,N) and hk14-KITL (C,G,K,O) transgenic mice and C57Bl/6 as wild-type control (D,H,L,P). (A-D) Transgenic and control mice. (E-H) Oil Red O staining of harderian gland of each mouse line at P2. (I-L) HE staining of harderian gland at P19. Blue arrows indicate melanocytes. (M-P) Fourteen-day cultures of P0 harderian gland on gelatin-coated dishes. (**Q**) Number of melanocytes per microscope field of the harderian gland sections. The data are averages from three different mice. *, $P<0.05$; **, $P<0.001$; ***, $P<0.00005$. (**R**) Number of colonies constituting more than 20 melanocytes from harderian glands. The data are averages from three different mice. *, $P<0.05$; **, $P<0.0005$. Scale bars in I-L: 50 μm.

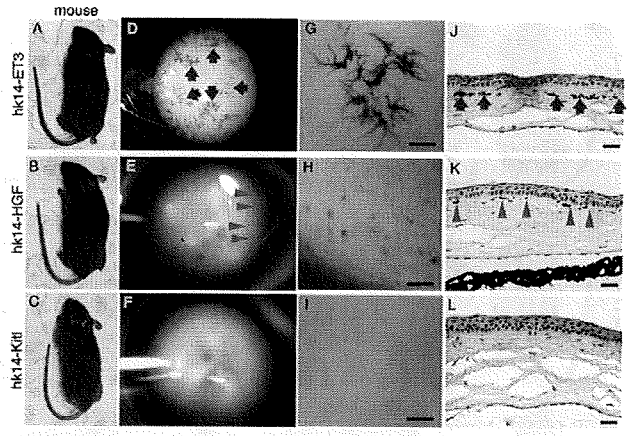

Fig. 5. Melanocytes in the cornea and the effect of exogenous expression of ET3, HGF and KITL. (**A,D,G,J**) hk14-ET3 transgenic mouse showing invasion of melanocytes into the cornea (arrows). (**B,E,H,K**) hk14-HGF transgenic mouse with the evidence of invasion of melanocyte-like, but not dendritic, pigmented cells into the cornea (arrowheads). (**C,F,I,L**) hk14-KITL transgenic mouse, showing no invasion of melanocytes into the cornea. Each transgenic mouse (A-C), its eye (D-F), cornea (G-I) and HE-stained corneal section (J-L) are shown. Scale bars: 50 μm.

hours revealed that black pigmented melanocytes present at the start of the culture did not divide actively (see Fig. S2A in the supplementary material). Pigmented cells marked in 36-hour cultures only divided once or twice in 264 hours (see Fig. S2B,C in the supplementary material). Thus, it is likely that the highly proliferative melanocyte lineage cells were not mature melanocytes and that the harderian gland or eye contained unpigmented melanoblasts. To further investigate the identity of these non-cutaneous melanoblasts, we tested whether the DCT-positive melanocyte lineage cells that were negative for the KIT receptor were really present as melanocyte precursors. For this purpose, transgenic mice were generated by crossing *Dct-Cre* knock-in mice [$Dct^{tm1(Cre)Bee}$] (Guyonneau et al., 2004) with CAG-CAT-EGFP reporter mice (Kawamoto et al., 2000) that express green fluorescent protein (GFP) under the control of a strong ubiquitous promoter (*CAG*) after Cre-mediated removal of a floxed chloramphenicol acetyl transferase (*CAT*) gene cassette so as to specifically label melanoblasts with GFP. Melanocyte lineage-specific GFP expression was confirmed in the transgenic mice, as described previously (Osawa et al., 2005). From these mice, we sorted 1000 GFP^+ cells from the $CD45^-/KIT^-$ gated population by FACS (Fig. 7C,D) and cultured them on ST2 monolayers for 14 days. From both harderian gland and ocular tissues, pigmented melanocytes were induced from the GFP^+ population; however, no melanocyte colony was detected from GFP^- cells in the $CD45^-/KIT^-$ population (Fig. 7E). Thus, precursors for the non-cutaneous melanocytes were mostly present as GFP^+ cells in the $CD45^-/KIT^-$ melanoblast population.

Factors responsible for the development of non-cutaneous melanocytes

To address the additional molecular signal(s) required for the growth and/or differentiation of melanocytes in non-cutaneous tissues, we tested the effect of signal inhibitors in vitro. First, we confirmed the effect of ET3 by using its receptor (EDNRB) antagonist, BQ788. When non-cutaneous melanocytes (i.e. those in harderian gland and eye) were cultured and treated with BQ788 or the ACK2 antibody, the growth and/or differentiation of the melanocytes was blocked effectively by BQ788 but not by ACK2 (Fig. 8A). Cutaneous melanocytes (i.e. epidermis) treated with the same concentration of these inhibitors totally disappeared (Fig. 8B). The numbers of melanocytes derived from the harderian gland and uvea were partially reduced by ACK2 treatment, but were stably maintained over a 1-50 μg/ml concentration range (Fig. 8C,D); by contrast, the number of melanocytes derived from the epidermis was sharply reduced at higher ACK2 concentrations (Fig. 8E). These results are consistent with those shown in Fig. 2, which indicated that non-cutaneous melanocytes can survive when treated with an amount of ACK2 that is effective in blocking the cutaneous melanocytes.

To investigate whether there are factors crucial for the growth and differentiation of non-cutaneous melanocytes in addition to KITL and ET3, we added various inhibitors to melanocyte cultures

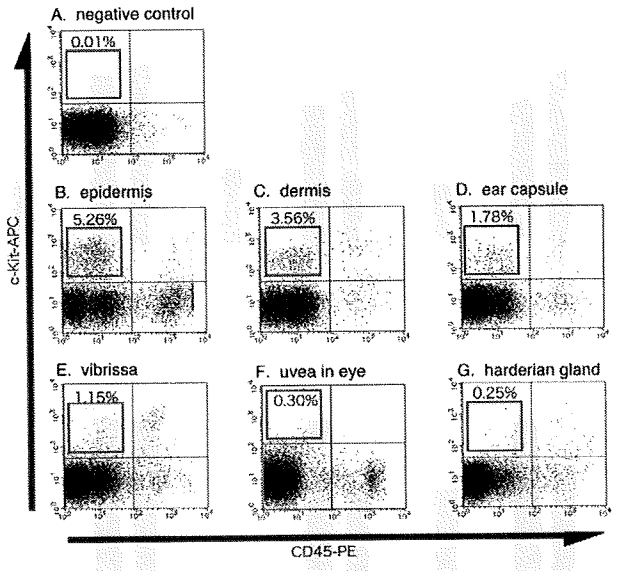

Fig. 6. Flow cytometric analysis and cell sorting of KIT⁺/CD45⁻ cells from cutaneous and non-cutaneous tissues. (**A-G**) By use of KIT-APC and CD45-PE, the percentage of KIT⁺/CD45⁻ cells (melanoblasts) was analyzed in the epidermis (B), dermis (C), ear capsule (D), vibrissa (E), uvea (F) and harderian gland (G); A shows a negative control.. The percentage of KIT⁺/CD45⁻ cells is shown in the top-left quadrant of each panel.

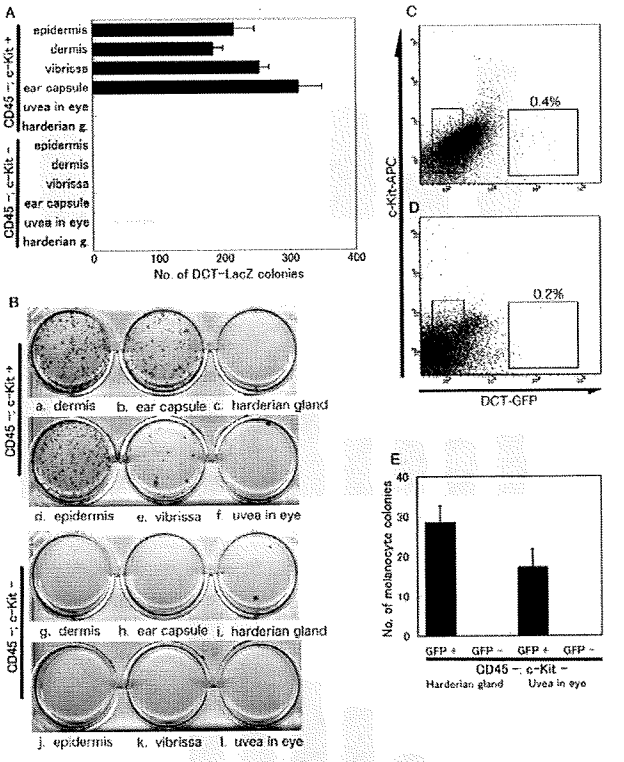

Fig. 7. In vitro differentiation of KIT⁺/CD45⁻ melanoblasts. (**A**) Number of DCT-lacZ-positive colonies generated after 14 days in cultures started from 1000 KIT⁺/CD45⁻ or KIT⁻/CD45⁻ cells sorted from the indicated tissues of P0 mice. (**B**) Dishes representative of the data shown in A. One thousand KIT⁺/CD45⁻ (**a-f**) or KIT⁻/CD45⁻ (**g-l**) cells purified by cell sorting were inoculated onto a monolayer of ST2 stromal cells. KIT⁺/CD45⁻ cells, but not KIT⁻/CD45⁻ cells, included melanoblasts in the dermis (a,g), ear capsule (b,h), epidermis (d,j) and vibrissae (e,k), but not in non-cutaneous tissue [harderian gland (c,i), uvea (f,l)]. The uvea and harderian gland contained fewer than one cell per thousand that generated DCT-lacZ-positive colonies in vitro. (**C,D**) Flow cytometric analysis of GFP⁺ cells among the KIT⁻/CD45⁻ cells in the harderian gland (C) and uvea (D). The percentage of GFP⁺ cells in the KIT⁻/CD45⁻ fractions in each panel is shown. (**E**) Number of melanocyte colonies derived from 1000 sorted cells from the GFP⁺ or GFP⁻ populations indicated in C and D.

prepared from P0 DCT-lacZ mice. When melanocytes from the harderian gland were cultured and exposed to an effective amount of PD98059, which is a MEK kinase inhibitor, or to a MET kinase inhibitor that inhibits HGF signaling, their growth and/or differentiation was severely inhibited (Fig. 9). PD98059 was effective toward all melanocyte populations tested (Fig. 9). However, the MET kinase inhibitor was more suppressive toward melanocytes from non-cutaneous tissues (Fig. 9E,F) than toward those from cutaneous tissues (Fig. 9A-D), indicating a role for HGF in the development of non-cutaneous melanocytes. Other inhibitors tested, including γ-secretase inhibitor, VEGFR (KDR) inhibitor (SU1498), FGFR inhibitor (SU5402), EGFR inhibitor (AG1433), p38 (MAPK14) inhibitor (SB203580) and Rho/Rock inhibitor (Y27632), did not show a statistically significant inhibitory effect on the melanocyte populations tested (see Fig. S3 in the supplementary material).

Further evidence for distinct epidermal and dermal melanocyte cell types

In the melanocytosis model hk14-ET3 and hk14-HGF transgenic mice, the melanocytes were maintained mostly in the dermis, whereas those in hk14-KITL transgenic mice were restricted to the epidermis, even in the aged individuals (Fig. 3E-L). Interestingly, when hk14-ET3 or hk14-HGF mice were crossed with hk14-KITL mice, the melanocytes of the double-transgenic mice were distributed to both dermis and epidermis, as a simple superimposition of both phenotypes (Fig. 10A,B). It could be that if dermal and epidermal melanocytes and their precursors maintained in the skin were mutually compatible, i.e. dermal melanocyte precursors could be recruited to become epidermal melanocytes by the exogenous ET3, an imbalance of dermal and epidermal melanocyte distribution might occur. Thus, the phenotype of the double-transgenic mice suggests the fairly discriminate and independent maintenance of these two melanocyte populations.

When a hk14-ET3 or hk14-HGF mouse was crossed with a Kit^{V620A}Tg piebaldism model mouse, the coat color pattern of the double-transgenic hk14-ET3/+;Kit^{V620A}/+ Tg or hk14-HGF/+;Kit^{V620A}/+ Tg mice was indistinguishable from that of Kit^{V620A}/+ Tg or Kit^{V620A}/Kit^{V620A} Tg mice (Fig. 11D,I). However, the skin of the double-transgenic mice was heavily pigmented, even in the area covered with white hair (Fig. 11E,J). The characteristic, heavily pigmented skin pattern of hk14-ET3 and hk14-HGF mice, and the characteristic white spot of the central head region and coat color of Kit^{V620A}Tg mice, did not change during the postnatal stage (Fig. 11A-D,F-I) (Tosaki et al., 2006). Histological analysis revealed that the dermal skin of hk14-ET3/+;Kit^{V620A}/+ Tg or hk14-HGF/+;Kit^{V620A}/+ Tg mice was pigmented (Fig. 11K,L), whereas the epidermis was not. By contrast, hk14-KITL/+;Kit^{V620A}/+ Tg

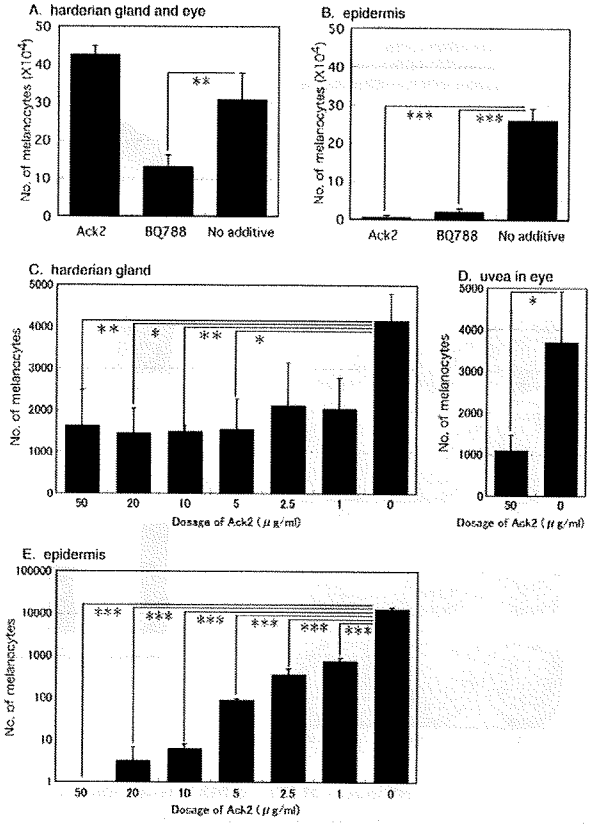

Fig. 8. Culture of P0 melanocytes with ACK2 or BQ788. (**A**,**B**) The number of melanocytes after 14 days of culturing 100,000 cells from epidermis (B) and harderian gland and uvea (A) seeded on gelatin-coated dishes and treated with effective amounts of ACK2 or BQ788. (**C-E**) ACK2 dose independency of non-cutaneous melanocytes (C, harderian gland; D, uvea) compared with the dose dependency for cutaneous melanocytes (E, epidermis). *, $P<0.05$; **, $P<0.01$; ***, $P<0.001$.

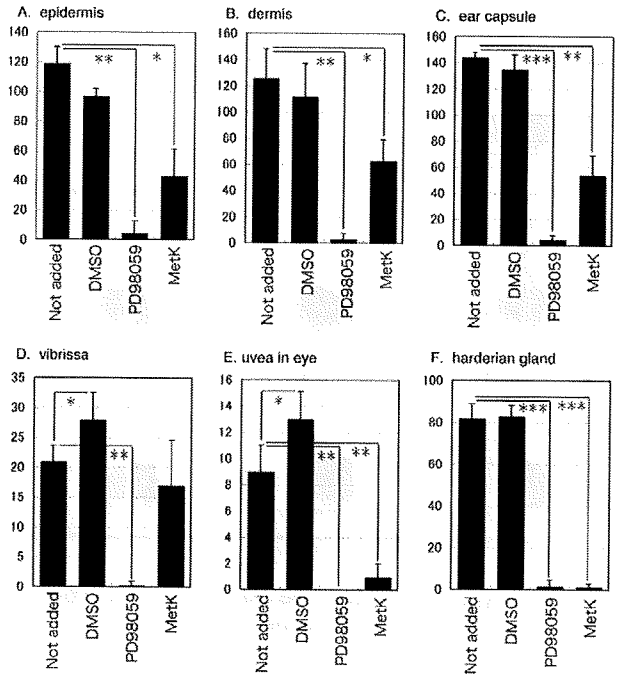

Fig. 9. Effect of inhibitors on melanocytes of various sources. Ten thousand cells from the epidermis (**A**), dermis (**B**), ear capsule (**C**), vibrissa (**D**), uvea (**E**), and harderian gland (**F**), were seeded onto monolayers of ST2 cells, and PD98059, MET kinase inhibitor (Metk), DMSO (as a vehicle control) or nothing (Not added) was added. After 14 days, the number of DCT-lacZ-positive colonies was counted. The average of three independent experiments is shown. *, $P<0.05$; **, $P<0.01$; ***, $P<0.001$.

mice with similar white spots showed pigmented skin under the black hair and totally unpigmented skin under the white hair (Fig. 11M-O). These results indicate that the ectopic localization of melanocytes in the dermis is induced and maintained by the expression of ET3 or HGF in the skin and that these dermal melanocytes do not contribute to hair pigmentation. These observations allow us to conclude that cutaneous melanocytes can be classified into two types, one being epidermal melanocytes, which are highly dependent on KIT, and the other being dermal melanocytes, which are more responsive to ET3 and HGF. As judged by their response to these factors, dermal melanocytes share the characteristics of non-cutaneous melanocytes found in the harderian glands and uvea of the eye.

DISCUSSION

Melanocytes are generally classified into cutaneous and non-cutaneous (extra-cutaneous) types. Cutaneous melanocytes are pathophysiologically distinguished as epidermal and dermal melanocytes. In this report, we described non-cutaneous melanocytes that developed in the eye, ear and harderian gland that were highly dependent on ET3 and HGF signaling and less dependent (although not totally independent) on KIT signaling, and, by contrast, epidermal melanocytes that were more dependent on KIT signaling. Cutaneous melanocytes in the dermis were revealed to be more selectively responsive to ET3 and HGF, like non-cutaneous melanocytes, and could be distinguished from epidermal melanocytes by not contributing to hair pigmentation.

In the context of the structure of skin tissue, the epidermis and dermis are composed of completely different cell populations, and therefore the cells distributed to these two regions are supposedly different in their molecular components, such as adhesion molecules, and in their growth signal dependency. Skin dendritic cells are classified into epidermal Langerhans cells and dermal dendritic cells based on differences in their cell surface marker expression patterns, gene expression profiles, growth signal requirements and immunological functions (Steinman et al., 1997). In the case of melanocytes, the expression of transgenes such as *Et3* or *Hgf* (Fig. 3) could have induced a permanent maintenance of dermal melanocytes that normally disappear after birth, indicating the specific growth requirements of dermal melanocytes. In other words, if dermal and epidermal melanocytes are of an identical cell lineage and are arbitrarily distributed among the skin tissues, then melanocyte distribution in the *Kitl* transgenic skin should have been similar to that in the *Et3* and *Hgf* transgenic mice.

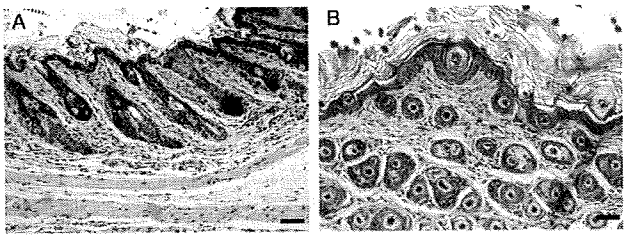

Fig. 10. Skin phenotypes of hk14-ET3/+;hk14-KITL/+ and hk14-HGF/+;hk14-KITL/+ double-transgenic mice. Skin samples from hk14-ET3/+;hk14-KITL/+ (**A**) and hk14-HGF/+;hk14-KITL/+ (**B**) double-transgenic mice were sectioned and stained with HE. Both of these double transgenic mice contain dermal and epidermal melanocytes Scale bars: 50 μm.

Dark skin (DSK) mutant mice also support our notion of distinct types of melanocyte because these mice are classified into dermal and epidermal DSK types (Fitch et al., 2003; Van Raamsdonk et al., 2004). Importantly, no DSK mutant mice are known to contain melanocytes in both their epidermis and dermis, indicating factor-specific localization of skin melanocytes. In accordance with our results, *Dsk3* and *Dsk4* (*Rps19* and *Rps20*) mutants would contain epidermal melanocytes generated by the augmented expression of skin KITL (McGowan et al., 2008). Recent identification of the uveal melanoma and blue naevi-specific mutation of the human counterpart of DSK1 (GNAQ), the heterotrimeric G-protein α-subunit, as opposed to the BRAF and NRAS mutations exclusively found in neoplasms originating from epidermal melanocytes (Van Raamsdonk et al., 2009), also indicate the distinct nature of non-cutaneous and epidermal melanocytes. Still, as suggested by Van Raamsdonk et al. (Van Raamsdonk et al., 2004), increased ET3 or HGF signaling might cause excessive proliferation of the early melanoblasts, followed by their restricted entry into the epidermis across the basal layer. In this scenario, melanocytes left behind in the dermis may develop into the dermal cell type in response to dermal-specific environmental cues.

The precise origins of the non-cutaneous and dermal melanocytes, as well as of epidermal melanocytes, are still open to further investigation. Epidermal melanocytes, including those of hair follicles, are maintained in a KITL-rich environment, whereas dermal melanocytes are supposed to be selectively maintained by

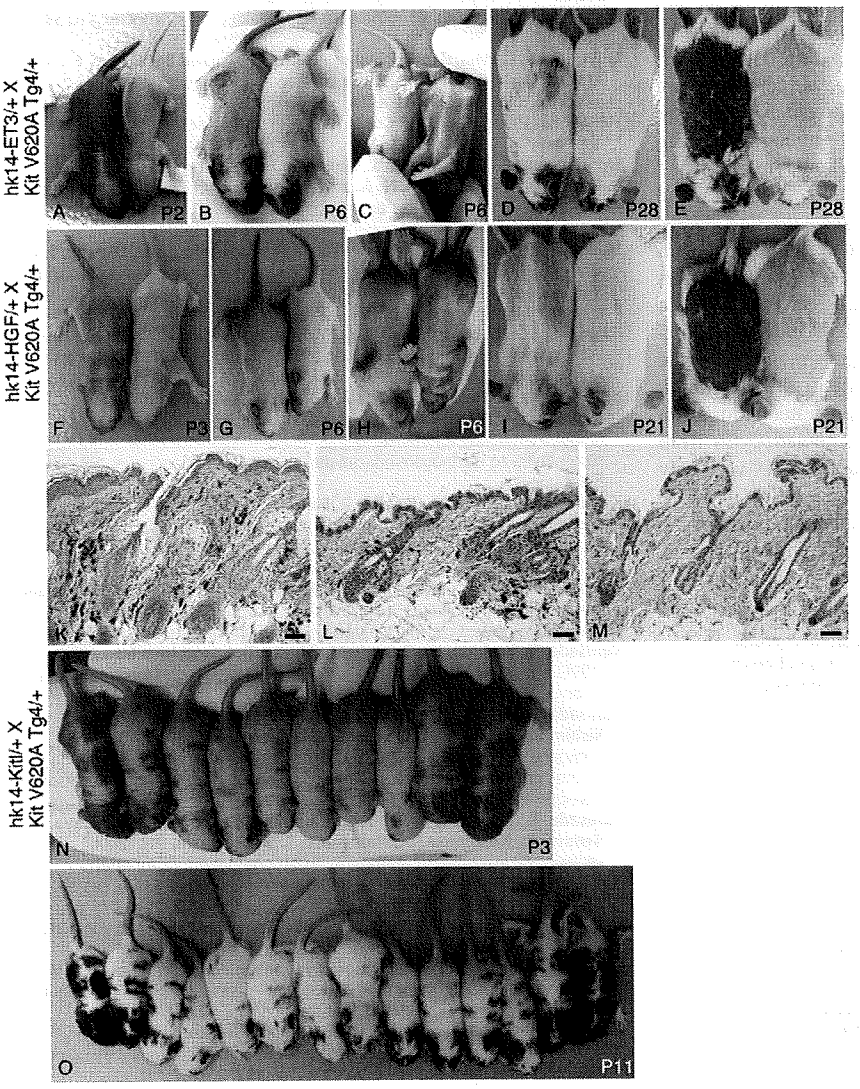

Fig. 11. Mice with pigmented dermis and white hair. (**A-E**) Mice with black pigmented dermis and white hair derived from a cross between hk14-ET3/+ and Kit V620A Tg4/+ mice (left pup in A,B,D,E and right pup in C). Photographs were taken at P2, P6 and P28 as labeled. Kit V620A Tg4/+ mice are shown alongside the double-transgenic mice. (**F-J**) Mice with black pigmented dermis and white hair derived from a cross between hk14-HGF/+ and Kit V620A Tg4/+ mice (left pup in F,G,I,J and right pup in H). Photographs were taken at P3, P6 and P21 as labeled. Kit V620A Tg4/+ mice are shown alongside the double-transgenic mice. (**K-M**) HE-stained skin samples from hk14-ET3/+;Kit V620A Tg4/+ (K) and hk14-HGF/+;Kit Tg4/+ (L) mice clearly show the absence of pigment granules in hair follicles but the presence of melanocytes in dermis, whereas hk14-KITL/+;Kit V620A Tg4/+ (M) samples show the absence of both pigment granules in hair follicles and melanocytes in dermis under the white hair. (**N,O**) Mice with black pigmented epidermis and black hair derived from a cross between hk14-KITL/+ and Kit V620A Tg4/+ mice. Photographs were taken at P3 and P11 as labeled. Scale bars: 50 μm.

ET3 or HGF expression. Since the number of epidermal melanocytes and their distribution pattern were not affected by ET3 or HGF expression (Kunisada et al., 1998; Kunisada et al., 2000) (H.A. and T.K., unpublished), common precursors for these two melanocyte populations would probably have separated from each other at a considerably early developmental stage. If not, common precursors would have been exhaustively used for the dermal melanocyte population. In addition, hk14-ET3/+;Kit^{V620A}/+ Tg mice are white in coat color and have dark pigmented dermal skin underneath, suggesting that dermal- and epidermal-restricted niches are required for each melanocyte population. This lifetime-stable localization further supports the distinct nature of these two populations. Recently, Notch signaling was reported to be selectively employed for the maintenance of epidermal melanocytes: in *Notch1* and/or *Notch2* conditional knockout mice, the ear and choroid layer were pigmented normally, in contrast to the gradual loss of coat color pigmentation (Schouwey et al., 2007). This finding also highlights the discrimination of epidermal melanocytes from dermal or non-cutaneous melanocytes.

In relation to skin diseases caused by aberrant melanocyte development, the characteristics of the melanocytes should be considered. In the case of dermal melanocytosis, a broad group of congenital and acquired melanocytic lesions (Zembowicz and Mihm, 2004), ET or HGF are more likely to be involved in the pathogenesis of this disease than is KIT signaling. However, it should also be emphasized that both melanocyte cell types are derived from common neural crest-derived precursors, as *W/W* mutation or extensive blockade of KIT signaling during embryogenesis completely eliminates the melanocytes from the whole body. In fact, we occasionally found W^v/W^v mice with white ear capsules accompanied by totally unpigmented harderian glands, in contrast to the majority of the W^v/W^v individuals with pigmentation in both their ear capsules and harderian glands (as shown in Fig. 1C). This finding might indicate a decisive effect of a small fluctuation in the KIT signal among W^v/W^v individuals, i.e. reflecting an exacting threshold of KIT signal intensity for the survival of developing melanocytes, at least in their common precursors. At the same time, we demonstrated the strict discrimination of non-cutaneous and dermal melanocytes from epidermal melanocytes based on their reactions to variously manipulated external ligands, including KITL, ET3 and HGF. These findings might help towards a clearer understanding of the pathogenesis of melanocyte-related diseases, including melanomas.

Acknowledgements

We thank Dr Shin-ichi Nishikawa for providing the ACK2 hybridoma cell line and ST2 stromal cell line, Kyoko Takahashi for her excellent technical assistance, and Drs Hisahiro Yoshida, Tsutomu Motohashi and Kenichi Tezuka for their thoughtful advice. This work was supported by JSPS Research Fellowships for Young Scientists to H.A.

Supplementary material

Supplementary material for this article is available at http://dev.biologists.org/cgi/content/full/136/15/2511/DC1

References

Aoki, H., Motohashi, T., Yoshimura, N., Yamazaki, H., Yamane, T., Panthier, J. J. and Kunisada, T. (2005). Cooperative and indispensable roles of endothelin 3 and KIT signalings in melanocyte development. *Dev. Dyn.* **233**, 407-417.

Aoki, H., Yoshida, H., Hara, A., Suzuki, T. and Kunisada, T. (2008a). Transplantation of melanocytes into iris: method for iris repigmentation. *Transplantation* **85**, 492-494.

Aoki, H., Hara, A., Motohashi, T., Chem, H. and Kunisada, T. (2008b). Iris as a recipient tissue for pigment cells: organized in vivo differentiation of melanocytes and pigmented epithelium derived from embryonic stem cells in vitro. *Dev. Dyn.* **237**, 2394-2404.

Aoki, H., Hara, A., Niwa, M., Motohashi, T., Suzuki, T. and Kunisada, T. (2008c). Transplantation of cells from eye-like structures differentiated from embryonic stem cells in vitro and in vivo regeneration of retinal ganglion-like cells. *Graefes. Arch. Clin. Exp. Ophthalmol.* **246**, 255-265.

Aubin-Houzelstein, G., Djian-Zaouche, J., Bernex, F., Gadin, S., Delmas, V., Larue, L. and Panthier, J. J. (2008). Melanoblasts' proper location and timed differentiation depend on Notch/RBP-J signaling in postnatal hair follicles. *J. Invest. Dermatol.* **128**, 2686-2695.

Barsh, G. and Cotsarelis, G. (2007). How hair gets its pigment. *Cell* **130**, 779-781.

Baynash, A. G., Hosoda, K., Giaid, A., Richardson, J. A., Emoto, N., Hammer, R. E. and Yanagisawa, M. (1994). Interaction of endothelin-3 with endothelin-B receptor is essential for development of epidermal melanocytes and enteric neurons. *Cell* **79**, 1277-1285.

Boissy, R. E. (1999). Extracutaneous melanocytes. In *The Pigmentary System* (ed. J. J. Nordlund., R. E. Boissy., V. J. Hearing., R. A. King and J. P. Ortone), pp. 59-72. New York: Oxford University Press.

Botchkareva, N. V., Khlgatian, M., Longley, B. J., Botchkarev, V. A. and Gilchrest, B. A. (2001). SCF/c-kit signaling is required for cyclic regeneration of the hair pigmentation unit. *FASEB J.* **15**, 645-658.

Cable, J., Jackson, I. J. and Steel, K. P. (1995). Mutations at the W locus affect survival of neural crest-derived melanocytes in the mouse. *Mech. Dev.* **50**, 139-150.

Dorsky, R. I., Raible, D. W. and Moon, R. T. (2000). Direct regulation of nacre, a zebrafish MITF homolog required for pigment cell formation, by the Wnt pathway. *Genes Dev.* **14**, 158-162.

Fitch, K. R., McGowan, K. A., van Raamsdonk, C. D., Fuchs, H., Lee, D., Puech, A., Hérault, Y., Threadgill, D. W., Hrabé de Angelis, M. and Barsh, G. S. (2003). Genetics of dark skin in mice. *Genes Dev.* **17**, 214-228.

Geissler, E. N., Ryan, M. A. and Housman, D. E. (1988). The dominant-white spotting (W) locus of the mouse encodes the c-kit proto-oncogene. *Cell* **55**, 185-192.

Guyonneau, L., Murisier, F., Rossier, A., Moulin, A. and Beermann, F. (2004). Melanocytes and pigmentation are affected in dopachrome tautomerase knockout mice. *Mol. Cell. Biol.* **24**, 3396-3403.

Hall, B. K. (1999). *The Neural Crest in Development and Evolution*. New York: Springer.

Hodgkinson, C. A., Moore, K. J., Nakayama, A., Steingrímsson, E., Copeland, N. G., Jenkins, N. A. and Arnheiter, H. (1993). Mutations at the mouse microphthalmia locus are associated with defects in a gene encoding a novel basic-helix-loop-helix-zipper protein. *Cell* **74**, 395-404.

Hosoda, K., Hammer, R. E., Richardson, J. A., Baynash, A. G., Cheung, J. C., Giaid, A. and Yanagisawa, M. (1994). Targeted and natural (piebald-lethal) mutations of endothelin-B receptor gene produce megacolon associated with spotted coat color in mice. *Cell* **79**, 1267-1276.

Ikeya, M., Lee, S. M., Johnson, J. E., McMahon, A. P. and Takada, S. (1997). Wnt signalling required for expansion of neural crest and CNS progenitors. *Nature* **389**, 966-970.

Inoue-Narita, T., Hamada, K., Sasaki, T., Hatakeyama, S., Fujita, S., Kawahara, K., Sasaki, M., Kishimoto, H., Eguchi, S., Kojima, I. et al. (2008). Pten deficiency in melanocytes results in resistance to hair graying and susceptibility to carcinogen-induced melanomagenesis. *Cancer Res.* **68**, 5760-5768.

Kawamoto, S., Niwa, H., Tashiro, F., Sano, S., Kondoh, G., Takeda, J., Tabayashi, K. and Miyazaki, J. (2000). A novel reporter mouse strain that expresses enhanced green fluorescent protein upon Cre-mediated recombination. *FEBS Lett.* **470**, 263-268.

Kos, L., Aronzon, A., Takayama, H., Maina, F., Ponzetto, C., Merlino, G. and Pavan, W. (1999). Hepatocyte growth factor/scatter factor-MET signaling in neural crest-derived melanocyte development. *Pigment Cell Res.* **12**, 13-21.

Kunisada, T., Yoshida, H., Ogawa, M., Shultz, D. L. and Nishikawa, S. I. (1996). Characterization and isolation of melanocyte progenitors from mouse embryos. *Dev. Growth Differ.* **38**, 87-97.

Kunisada, T., Yoshida, H., Yamazaki, H., Miyamoto, A., Hemmi, H., Nishimura, E., Shultz, L. D., Nishikawa, S. and Hayashi, S. (1998). Transgene expression of steel factor in the basal layer of epidermis promotes survival, proliferation, differentiation and migration of melanocyte precursors. *Development* **125**, 2915-2923.

Kunisada, T., Yamazaki, H., Hirobe, T., Kamei, S., Omoteno, M., Tagaya, H., Hemmi, H., Koshimizu, U., Nakamura, T. and Hayashi, S. I. (2000). Keratinocyte expression of transgenic hepatocyte growth factor affects melanocyte development, leading to dermal melanocytosis. *Mech. Dev.* **94**, 67-78.

Le Douarin, N. M. and Kalcheim, C. (1999). *The Neural Crest*, 2nd edn. New York: Cambridge University Press.

Lister, J. A., Robertson, C. P., Lepage, T., Johnson, S. L. and Raible, D. W. (1999). nacre encodes a zebrafish microphthalmia-related protein that regulates neural-crest-derived pigment cell fate. *Development* **126**, 3757-3767.

Mackenzie, M. A., Jordan, S. A., Budd, P. S. and Jackson, I. J. (1997). Activation of the receptor tyrosine kinase Kit is required for the proliferation of melanoblasts in the mouse embryo. *Dev. Biol.* **192**, 99-107.

Mak, S. S., Moriyama, M., Nishioka, E., Osawa, M. and Nishikawa, S. (2006). Indispensable role of Bcl2 in the development of the melanocyte stem cell. *Dev. Biol.* **291**, 144-153.
McGill, G. G., Horstmann, M., Widlund, H. R., Du, J., Motyckova, G., Nishimura, E. K., Lin, Y. L., Ramaswamy, S., Avery, W., Ding, H. F. et al. (2002). Bcl2 regulation by the melanocyte master regulator Mitf modulates lineage survival and melanoma cell viability. *Cell* **109**, 707-718.
McGill, G. G., Haq, R., Nishimura, E. K. and Fisher, D. E. (2006). c-Met expression is regulated by Mitf in the melanocyte lineage. *J. Biol. Chem.* **281**, 10365-10373.
McGowan, K. A., Li, J. Z., Park, C. Y., Beaudry, V., Tabor, H. K., Sabnis, A. J., Zhang, W., Fuchs, H., de Angelis, M. H., Myers, R. M. et al. (2008). Ribosomal mutations cause p53-mediated dark skin and pleiotropic effects. *Nat. Genet.* **40**, 963-970.
Moriyama, M., Osawa, M., Mak, S. S., Ohtsuka, T., Yamamoto, N., Han, H., Delmas, V., Kageyama, R., Beermann, F., Larue, L. et al. (2006). Notch signaling via Hes1 transcription factor maintains survival of melanoblasts and melanocyte stem cells. *J. Cell Biol.* **173**, 333-339.
Motohashi, T., Aoki, H., Chiba, K., Yoshimura, N. and Kunisada, T. (2007). Multipotent cell fate of neural crest-like cells derived from embryonic stem cells. *Stem Cells* **25**, 402-410.
Nakayama, A., Nguyen, M. T., Chen, C. C., Opdecamp, K., Hodgkinson, C. A. and Arnheiter, H. (1998). Mutations in microphthalmia, the mouse homolog of the human deafness gene MITF, affect neuroepithelial and neural crest-derived melanocytes differently. *Mech. Dev.* **70**, 155-166.
Nishikawa, S., Kusakabe, M., Yoshinaga, K., Ogawa, M., Hayashi, S., Kunisada, T., Era, T., Sakakura, T. and Nishikawa, S. (1991). In utero manipulation of coat color formation by a monoclonal anti-c-kit antibody: two distinct waves of c-kit-dependency during melanocyte development. *EMBO J.* **10**, 2111-2118.
Nishimura, E. K., Jordan, S. A., Oshima, H., Yoshida, H., Osawa, M., Moriyama, M., Jackson, I. J., Barrandon, Y., Miyachi, Y. and Nishikawa, S. (2002). Dominant role of the niche in melanocyte stem-cell fate determination. *Nature* **416**, 854-860.
Nishimura, E. K., Granter, S. R. and Fisher, D. E. (2005). Mechanisms of hair graying: incomplete melanocyte stem cell maintenance in the niche. *Science* **307**, 720-724.
Opdecamp, K., Nakayama, A., Nguyen, M. T., Hodgkinson, C. A., Pavan, W. J. and Arnheiter, H. (1997). Melanocyte development in vivo and in neural crest cell cultures: crucial dependence on the Mitf basic-helix-loop-helix-zipper transcription factor. *Development* **124**, 2377-2386.
Osawa, M. and Fisher, D. E. (2008). Notch and melanocytes: diverse outcomes from a single signal. *J. Invest. Dermatol.* **128**, 2571-2574.
Osawa, M., Egawa, G., Mak, S. S., Moriyama, M., Freter, R., Yonetani, S., Beermann, F. and Nishikawa, S. (2005). Molecular characterization of melanocyte stem cells in their niche. *Development* **132**, 5589-5599.
Pavan, W. J. and Tilghman, S. M. (1994). Piebald lethal (sl) acts early to disrupt the development of neural crest-derived melanocytes. *Proc. Natl. Acad. Sci. USA* **91**, 7159-7163.
Pingault, V., Bondurand, N., Kuhlbrodt, K., Goerich, D. E., Préhu, M. O., Puliti, A., Herbarth, B., Hermans-Borgmeyer, I., Legius, E., Matthijs, G. et al. (1998). SOX10 mutations in patients with Waardenburg-Hirschsprung disease. *Nat. Genet.* **18**, 171-173.
Potterf, S. B., Furumura, M., Dunn, K. J., Arnheiter, H. and Pavan, W. J. (2000). Transcription factor hierarchy in Waardenburg syndrome: regulation of MITF expression by SOX10 and PAX3. *Hum. Genet.* **107**, 1-6.
Sarin, K. Y. and Artandi, S. E. (2007). Aging, graying and loss of melanocyte stem cells. *Stem Cell Rev.* **3**, 212-217.
Schouwey, K., Delmas, V., Larue, L., Zimber-Strobl, U., Strobl, L. J., Radtke, F. and Beermann, F. (2007). Notch1 and Notch2 receptors influence progressive hair graying in a dose-dependent manner. *Dev. Dyn.* **236**, 282-289.
Shin, M. K., Levorse, J. M., Ingram, R. S. and Tilghman, S. M. (1999). The temporal requirement for endothelin receptor-B signalling during neural crest development. *Nature* **402**, 496-501.
Southard-Smith, E. M., Kos, L. and Pavan, W. J. (1998). Sox10 mutation disrupts neural crest development in Dom Hirschsprung mouse model. *Nat. Genet.* **18**, 60-64.
Steinman, R. M., Pack, M. and Inaba, K. (1997). Dendritic cell development and maturation. *Adv. Exp. Med. Biol.* **417**, 1-6.
Tosaki, H., Kunisada, T., Motohashi, T., Aoki, H., Yoshida, H. and Kitajima, Y. (2006). Mice transgenic for Kit(V620A): recapitulation of piebaldism but not progressive depigmentation seen in humans with this mutation. *J. Invest. Dermatol.* **126**, 1111-1118.
Van Raamsdonk, C. D., Fitch, K. R., Fuchs, H., de Angelis, M. H. and Barsh, G. S. (2004). Effects of G-protein mutations on skin color. *Nat. Genet.* **36**, 961-968.
Van Raamsdonk, C. D., Bezrookove, V., Green, G., Bauer, J., Gaugler, L., O'Brien, J. M., Simpson, E. M., Barsh, G. S., Bastian, B. C. (2009). Frequent somatic mutations of GNAQ in uveal melanoma and blue naevi. *Nature* **457**, 599-602.
Watanabe, A., Takeda, K., Ploplis, B. and Tachibana, M. (1998). Epistatic relationship between Waardenburg syndrome genes MITF and PAX3. *Nat. Genet.* **18**, 283-286.
Wehrle-Haller, B. and Weston, J. A. (1995). Soluble and cell-bound forms of steel factor activity play distinct roles in melanocyte precursor dispersal and survival on the lateral neural crest migration pathway. *Development* **121**, 731-742.
Weiner, L., Han, R., Scicchitano, B. M., Li, J., Hasegawa, K., Grossi, M., Lee, D. and Brissette, J. L. (2007). Dedicated epithelial recipient cells determine pigmentation patterns. *Cell* **130**, 932-942.
Yamane, T., Hayashi, S., Mizoguchi, M., Yamazaki, H. and Kunisada, T. (1999). Derivation of melanocytes from embryonic stem cells in culture. *Dev. Dyn.* **216**, 450-458.
Yamazaki, H., Sakata, E., Yamane, T., Yanagisawa, A., Abe, K., Yamamura, K., Hayashi, S. and Kunisada, T. (2005). Presence and distribution of neural crest-derived cells in the murine developing thymus and their potential for differentiation. *Int. Immunol.* **17**, 549-558.
Yonetani, S., Moriyama, M., Nishigori, C., Osawa, M. and Nishikawa, S. (2008). In vitro expansion of immature melanoblasts and their ability to repopulate melanocyte stem cells in the hair follicle. *J. Invest. Dermatol.* **128**, 408-420.
Yoshida, H., Nishikawa, S.-I., Okamura, H., Sakakura, T. and Kusakabe, M. (1993). The role of c-kit proto-oncogene during melanocyte development in mouse. In vivo approach by the in utero microinjection of anti-c-kit antibody. *Dev. Growth Differ.* **35**, 209-220.
Yoshida, H., Kunisada, T., Kusakabe, M., Nishikawa, S. and Nishikawa, S. I. (1996a). Distinct stages of melanocyte differentiation revealed by analysis of nonuniform pigmentation patterns. *Development* **122**, 1207-1214.
Yoshida, H., Hayashi, S., Shultz, L. D., Yamamura, K., Nishikawa, S., Nishikawa, S. and Kunisada, T. (1996b). Neural and skin cell-specific expression pattern conferred by steel factor regulatory sequence in transgenic mice. *Dev. Dyn.* **207**, 222-232.
Yoshida, H., Kunisada, T., Grimm, T., Nishimura, E. K., Nishioka, E. and Nishikawa, S. I. (2001). Melanocyte migration and survival controlled by SCF/c-kit expression. *J. Investig. Dermatol. Symp. Proc.* **6**, 1-5.
Zembowicz, A. and Mihm, M. C. (2004). Dermal dendritic melanocytic proliferations: an update. *Histopathology* **45**, 433-451.

Oncogene (2009) 28, 3949–3959

www.nature.com/onc

ORIGINAL ARTICLE

Hypoxia promotes expansion of the CD133-positive glioma stem cells through activation of HIF-1α

A Soeda[1], M Park[1], D Lee[1], A Mintz[2], A Androutsellis-Theotokis[3], RD McKay[3], J Engh[2], T Iwama[4], T Kunisada[5], AB Kassam[1,2], IF Pollack[1,2] and DM Park[1,2,6]

[1]*Brain Tumor Program, University of Pittsburgh Cancer Institute, Pittsburgh, PA, USA;* [2]*Department of Neurological Surgery, University of Pittsburgh, Pittsburgh, PA, USA;* [3]*Laboratory of Molecular Biology, National Institutes of Health, Bethesda, MD, USA;* [4]*Department of Neurosurgery, Gifu University School of Medicine, Gifu, Japan;* [5]*Department of Tissue and Organ Development Regeneration and Advanced Medical Science, Gifu University School of Medicine, Gifu, Japan and* [6]*Department of Pharmacology and Chemical Biology, University of Pittsburgh, Pittsburgh, PA, USA*

Hypoxia contributes to the progression of a variety of cancers by activating adaptive transcriptional programs that promote cell survival, motility and tumor angiogenesis. Although the importance of hypoxia and subsequent hypoxia-inducible factor-1α (HIF-1α) activation in tumor angiogenesis is well known, their role in the regulation of glioma-derived stem cells is unclear. In this study, we show that hypoxia (1% oxygen) promotes the self-renewal capacity of CD133-positive human glioma-derived cancer stem cells (CSCs). Propagation of the glioma-derived CSCs in a hypoxic environment also led to the expansion of cells bearing CXCR4 (CD184), CD44^{low} and A2B5 surface markers. The enhanced self-renewal activity of the CD133-positive CSCs in hypoxia was preceded by upregulation of HIF-1α. Knockdown of HIF-1α abrogated the hypoxia-mediated CD133-positive CSC expansion. Inhibition of the phosphatidylinositol 3-kinase (PI3K)-Akt or ERK1/2 pathway reduced the hypoxia-driven CD133 expansion, suggesting that these signaling cascades may modulate the hypoxic response. Finally, CSCs propagated at hypoxia robustly retained the undifferentiated phenotype, whereas CSCs cultured at normoxia did not. These results suggest that response to hypoxia by CSCs involves the activation of HIF-1α to enhance the self-renewal activity of CD133-positive cells and to inhibit the induction of CSC differentiation. This study illustrates the importance of the tumor microenvironment in determining cellular behavior.
Oncogene (2009) **28,** 3949–3959; doi:10.1038/onc.2009.252; published online 31 August 2009

Keywords: glioma; cancer stem cell; HIF-1α; hypoxia; CD133

Correspondence: Dr DM Park, University of Pittsburgh Cancer Institute, UPMC Cancer Pavilion, 5th Floor, 5150 Centre Avenue, Pittsburgh, PA 15232, USA.
E-mail: parkdm@upmc.edu
Received 26 January 2009; revised 10 July 2009; accepted 25 July 2009; published online 31 August 2009

Introduction

Gliomas, the most common primary brain tumor, are believed to be initiated and maintained by cancer stem cells (CSCs), a population of cells capable of extensive self-renewal, differentiation into multiple lineages and recapitulation of the original tumor in immunodeficient mice (Galli *et al.*, 2004; Singh *et al.*, 2004). In that CSCs seem to have a central role in tumor initiation and recurrence, it has been suggested that definitive cancer treatment needs to target this population of cells (Reya *et al.*, 2001; Pardal *et al.*, 2003; Bao *et al.*, 2006a; Vescovi *et al.*, 2006; Park *et al.*, 2007). Similar to other cancers, microenvironmental interactions are believed to be critical in the pathogenesis and progression of gliomas (Calabrese *et al.*, 2007). As gliomagenesis and subsequent growth of the tumor may, in part, result from an aberrant interaction between the cancer cells and the tumor niche, a better understanding of the microenvironmental cues may lead to the identification of new therapeutic targets (Pouyssegur *et al.*, 2006; Keith and Simon, 2007; Calabrese *et al.*, 2007). Elucidating the tumorigenic role of the microenvironment may be as important as understanding the mechanisms involved in cellular transformation. Similar to the normal neural stem cell (NSC) niche in the subventricular zone, the CSC microenvironment of the glioma may provide the strictly regulated signals necessary to maintain the undifferentiated state of the CSCs, thereby preserving their proliferative and multipotential capacities (Pouyssegur *et al.*, 2006; Keith and Simon, 2007).

The proliferative phase leading to tumor expansion is thought to be governed by microenvironmental cues, including the regulation and availability of oxygen and nutrients (Keith and Simon, 2007). Although hypoxia may be an inevitable outcome of the rapidly growing tumor outstripping its vascular supply, it confers certain advantages on tumor cells (Pouyssegur *et al.*, 2006). For example, hypoxia renders tumor cells with greater resistance to anticancer therapy such as radiation. Therefore, factors that regulate the hypoxic state represent potential targets for anticancer therapy. Although the self-renewal capacity and the undifferentiated state of NSCs

are known to be enhanced by hypoxia (Gustafsson *et al.*, 2005; Chen *et al.*, 2007), such an effect on CSCs is unclear. One well-characterized mechanism of the cellular response to reduced oxygen availability involves the enhanced expression of the hypoxia-inducible factor-1α (HIF-1α) (Semenza and Wang, 1992; Maxwell *et al.*, 1997; Carmeliet *et al.*, 1998). HIF-1α has also been shown to be induced by numerous stimuli other than hypoxia, including insulin, insulin-like growth factors, epidermal growth factor (EGF) and heavy metals (Richard *et al.*, 1999; Zhong *et al.*, 2000; Fukuda *et al.*, 2002). In addition, the mammalian target of rapamycin (mTOR), a downstream effector of the PI3K pathway, is involved in hypoxic signal transduction and has been implicated in the regulation of HIF-1α stabilization, accumulation and activation (Hudson *et al.*, 2002).

We have shown earlier that EGF signaling promotes sphere formation and enhances the self-renewal capacity of CSCs, including the CD133-positive sub-population, a putative marker of glioma CSCs (Soeda *et al.*, 2008). In this study, we examined the role of hypoxia and the subsequent activation of HIF-1α in the self-renewal of human glioma-derived CSCs. The effect of hypoxia on CSCs was characterized by surface stem/progenitor and other marker expression including CD133, CD44, A2B5, CD24 and CXCR4 (CD184). We also investigated the regulation of HIF-1α by PI3K-Akt-mTOR and ERK/MAPK pathways in the glioma-derived CSCs. Furthermore, we characterized the differentiation state and the multipotential capacities of CSCs under normoxic and hypoxic conditions. Our data suggest hypoxia promotes self-renewal and proliferation of human glioma-derived CSCs, in part, by activation of HIF-1α, and that normoxia induces differentiation and restricts self-renewal of CSCs.

Results

Hypoxia enhances CD133+ CSC self-renewal and proliferation

All experiments were performed with previously established malignant-glioma-derived CSC lines from freshly resected surgical specimens under a protocol approved by the local Institutional Review Board (Oka *et al.*, 2007; Soeda *et al.*, 2008). These CSC lines express markers of the undifferentiated phenotype, show self-renewal and are multipotent. These cells express the neural stem/progenitor markers such as nestin, musashi-1 and CD133 in the presence of EGF in serum-free medium. Transplantation of 100–1000 CD133-positive cells into the brains of immunodeficient mice recapitulates the original tumor (Oka *et al.*, 2007). These cells also express markers of neuronal, astrocytic and oligodendroglial lineages in serum containing differentiation medium (Supplementary Figure 1). The self-renewal capacities of these cells were determined using a modified sphere-forming assay (Soeda *et al.*, 2008). At hypoxic condition (1% oxygen), the sphere-forming abilities of the dissociated single cells were strikingly increased compared with normoxia (Figure 1a). Analysis of the CD133+/CD133− ratio showed that hypoxia preferentially expanded the CD133+ CSCs in a time-dependent manner (Figures 1b–d).

Hypoxia promotes expression of HIF-1α and vascular endothelial growth factor

In that HIF-1α is an important molecule in the response of cells to hypoxia, we hypothesized that hypoxia may promote the self-renewal of the CD133-positive CSCs by stabilizing HIF-1α expression. To test this hypothesis, we cultured tumor spheres in hypoxia and determined HIF-1α expression by western blot (Figure 2a). At 1% oxygen condition, HIF-1α was observed within 2 h. Interestingly, there was no difference in HIF-2α expression. As vascular endothelial growth factor (VEGF) is an important paracrine growth factor involved in angiogenic response to HIF-1α, we determined the VEGF levels at normoxia and hypoxia. After exposure to hypoxia for 72 h, the VEGF levels were nearly threefold higher in hypoxia. Interestingly, CSCs derived from grade III glioma (X03) produced less VEGF compared with grade IV-derived CSCs (X01 and X02).

We used a transient knockdown approach to further investigate the role of HIF-1α, HIF-2α, prolyl hydroxylase domain-containing protein-2 (PHD2) and Notch1 in promoting the sphere-forming capacity of glioma CSCs. Transfection of CSCs propagated in hypoxia with HIF-1α small interfering RNA (siRNA) abrogated the expression of HIF-1α and decreased the CD133-positive sub-population (Figure 2c). This also resulted in inhibition of sphere formation (Figure 2c). HIF-1α depletion experiment performed at normoxia had no effect on CSC sphere-forming capacity (data not shown). PHD2 depletion at normoxia resulted in low expression of HIF-1α (Figure 2d). However, this did not lead to a significant difference in sphere formation. Depletion of HIF-2α and Notch1 also showed no difference in the sphere-forming ability (Figures 2e and f). These data suggest that for the X01, X02 and X03 CSC lines, hypoxia is a potent inducer of HIF-1α expression, and that HIF-1α has a critical role in hypoxia-mediated self-renewal.

Hypoxia-induced expression of HIF-1α is augmented by the EGFR signaling pathway

Epidermal growth factor receptor (EGFR) signaling is important to the survival and growth of glioma cells. We have shown earlier that soluble EGF enhances the self-renewal capacity of CD133-positive CSCs in a dose-dependent manner. To determine the combined effect of hypoxia and EGFR signaling, recombinant EGF was added to CSCs propagated at normoxia and hypoxia. The addition of EGF to CSCs in normoxia had no effect on HIF-1α. However, EGF was capable of further amplifying the hypoxia-induced expression of HIF-1α, suggesting that EGFR signaling may have the potential to augment the hypoxia-mediated CSC self-renewal

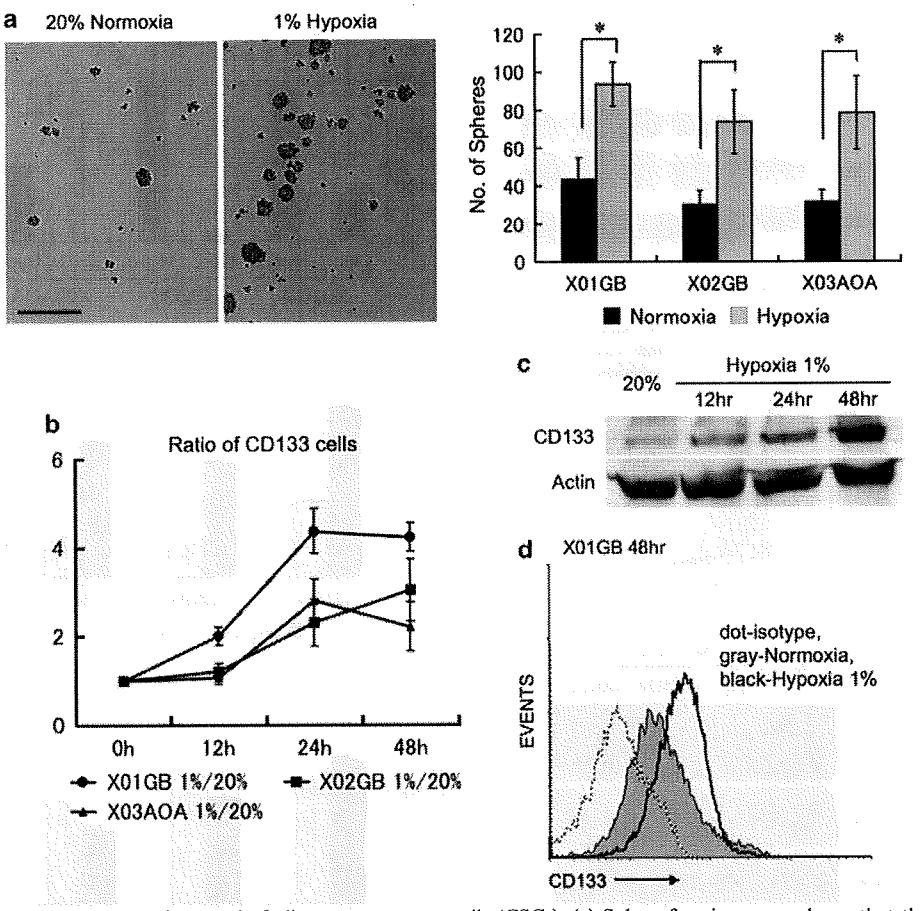

Figure 1 Hypoxia promotes self-renewal of glioma cancer stem cells (CSCs). (**a**) Sphere-forming assay shows that the self-renewal capacity of CSCs is increased when incubated at 1% oxygen (hypoxia) compared with 20% oxygen. CSCs cultured in serum-free medium supplemented with epidermal growth factor (20 ng/ml) were incubated for 5 days. On the left, the picture of cells in a representative well was taken with phase contrast microscopy. On the right, the *X* axis of the graph indicates different CSC lines, and the *Y* axis indicates the number of spheres present. Using a 24-well plate format, one thousand cells were seeded per plate in 2 ml medium, and the number of spheres was counted after 5 days. The results shown in the graph are mean ± s.d. from three experiments. $*P<0.05$, bar = 100 μm. (**b**) The relative number of CD133-positive cells increases in response to hypoxia. The graph shows the relative expansion of CD133-positive cells as determined by a ratio of CD133-positive cells to CD133-negative cells at hypoxia versus normoxia at different time points. The increasing ratio implies a specific expansion of CD133-positive cells rather than a nonspecific expansion because of the overall increase in total cell number. (**c**) Representative immunoblot for X01 CSC line shows increasing expression of CD133 total protein level in a time-dependent manner under hypoxia. (**d**) Representative fluorescence-activated cell sorting histogram for the X01CSC line shows an expansion of CD133-positive cells in hypoxia.

capacity (Figure 3a). Yet, in the absence of exogenous EGF, hypoxia alone was able to expand the CD133-positive CSCs (Figure 3b). These observations suggest the presence of cross talk between the hypoxic response and EGFR signaling, but the latter is not required for hypoxia-induced expansion of CD133-positive CSCs.

PI3K/Akt/mTOR and ERK pathways interact with hypoxia signaling

Hypoxia is capable of stimulating key signaling pathways activated in stem cells and cancer (Keith and Simon, 2007). In the absence of exogenous EGF, hypoxia alone was sufficient to activate the PI3K and MAPK pathways in the CSCs by augmenting phosphorylation of Akt, ERK and p70S6-kinase (Figure 4a). To further characterize the cross talk between the growth factor and hypoxia signaling pathways in the glioma-derived CSCs, cells cultured at hypoxia were exposed to various inhibitors: PI3K inhibitor (LY294002), ERK inhibitor (PD98059) and mTOR inhibitor (rapamycin). Cells were pretreated with the inhibitors for 2 h before placement in the 1% oxygen environment. Hypoxic induction of HIF-1α was attenuated by these inhibitors (Figure 4b). Finally, we investigated the effect of such inhibitors on the hypoxia-induced CD133-positive CSC expansion. Inhibition of the PI3K and ERK pathways independently abrogated the HIF-1α-mediated expansion of CD133-positive CSCs (Figure 4c). These data suggest that inhibition of the growth factor signaling pathway may attenuate hypoxia-induced expansion of CD133-positive CSCs.

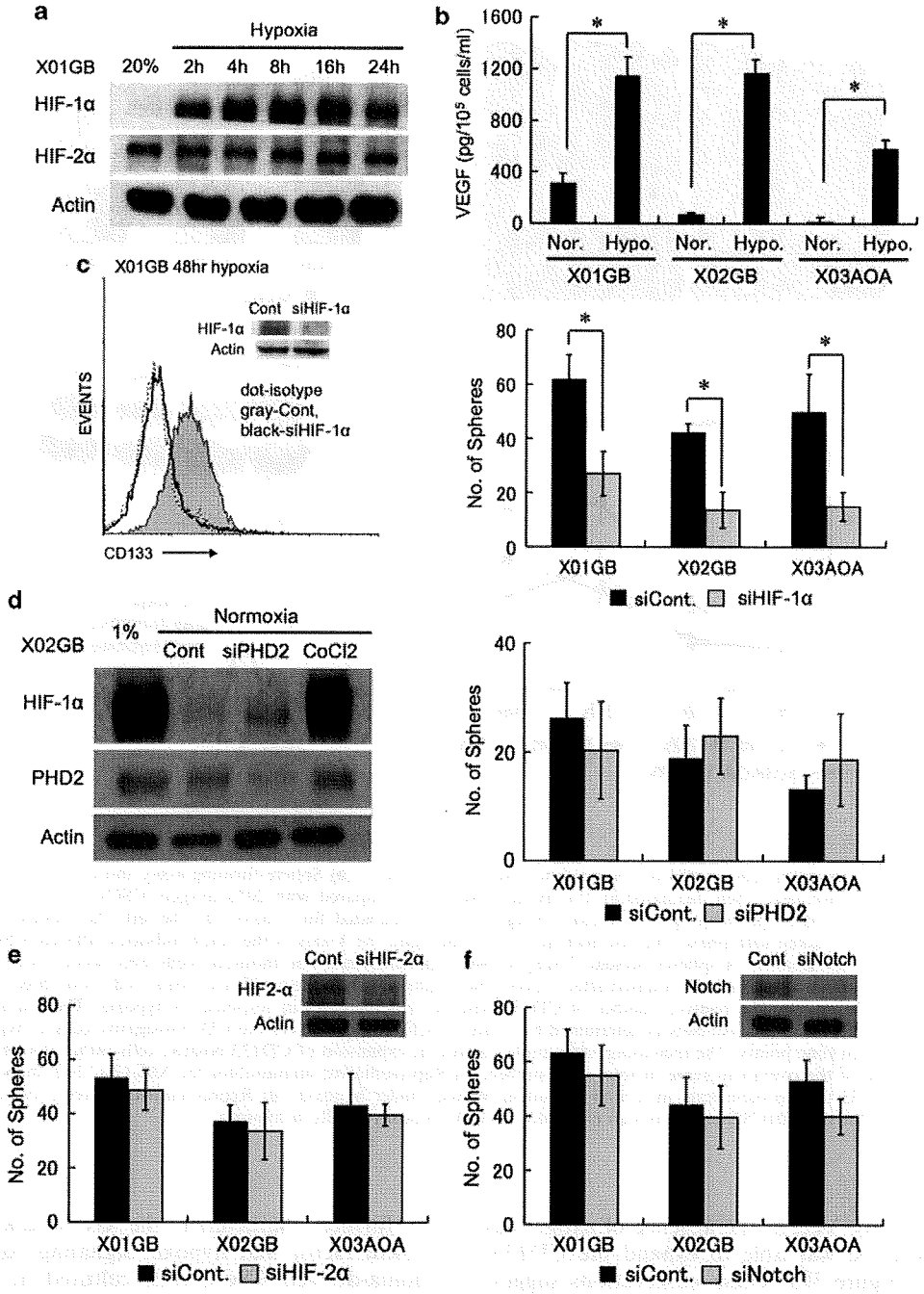

Figure 2 Hypoxia-inducible factor-1α (HIF-1α) and vascular endothelial growth factor (VEGF) expressions under hypoxic condition. (**a**) HIF-1α expression level is seen at hypoxia in a time-dependent manner. HIF-2α expression appears stable and unaffected by oxygen tension in the X01 cancer stem cell (CSC) line. (**b**) Hypoxia promotes VEGF production by CSCs. The results shown in the graph are mean ± s.d. from three experiments. $*P<0.05$. (**c**) Treatment of CSCs with HIF-1α small interfering RNA (siRNA) abrogates the induction of HIF-1α protein in response to hypoxia and decreases CD133 expression. The adjacent graph on the right shows that the depletion of HIF-1α results in a striking reduction in the sphere-forming capacity. Data are from representative experiments repeated three times. (**d**) Depletion of prolyl hydroxylase domain-containing protein-2 (PHD2) induces expression of HIF-1α at normoxia, but does not show enhanced sphere formation. PHD2 inhibition with siPHD2 at room oxygen tension results in low expression of HIF-1α. However, there is no significant difference in sphere formation. (**e** and **f**) Depletion of neither HIF-2α nor Notch1 affects the sphere-forming capacity.

Propagation at hypoxia expands the CD133/CXCR4/CD44^{low}/A2B5/CD24-positive cells

To further characterize the phenotype of the CSC subpopulation showing expansion at reduced oxygen, we performed fluorescence-activated cell sorting analysis of CSCs with a series of surface markers associated with stem/progenitor and cancer cells. The effect of hypoxia on the differential expressions of CD133, CXCR4

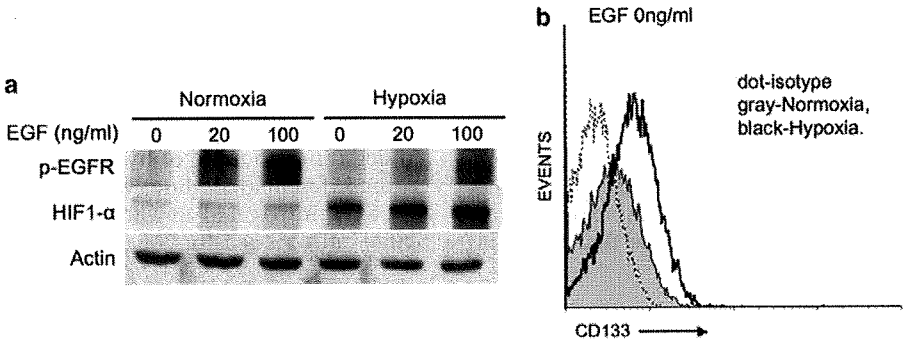

Figure 3 Hypoxia-inducible factor-1α (HIF-1α) induction by hypoxia is amplified by epidermal growth factor receptor (EGFR) signaling, but is not required. (**a**) HIF-1α proteins were analysed by western blotting experiments with different concentrations of EGF (0, 20, 100 ng/ml) at normoxia and hypoxia. (**b**) Fluorescence-activated cell sorting analysis shows that hypoxia is capable of expanding the CD133-positive cancer stem cell (X01 line) in the absence of exogenous EGF ligand. Data are from representative experiments repeated three times.

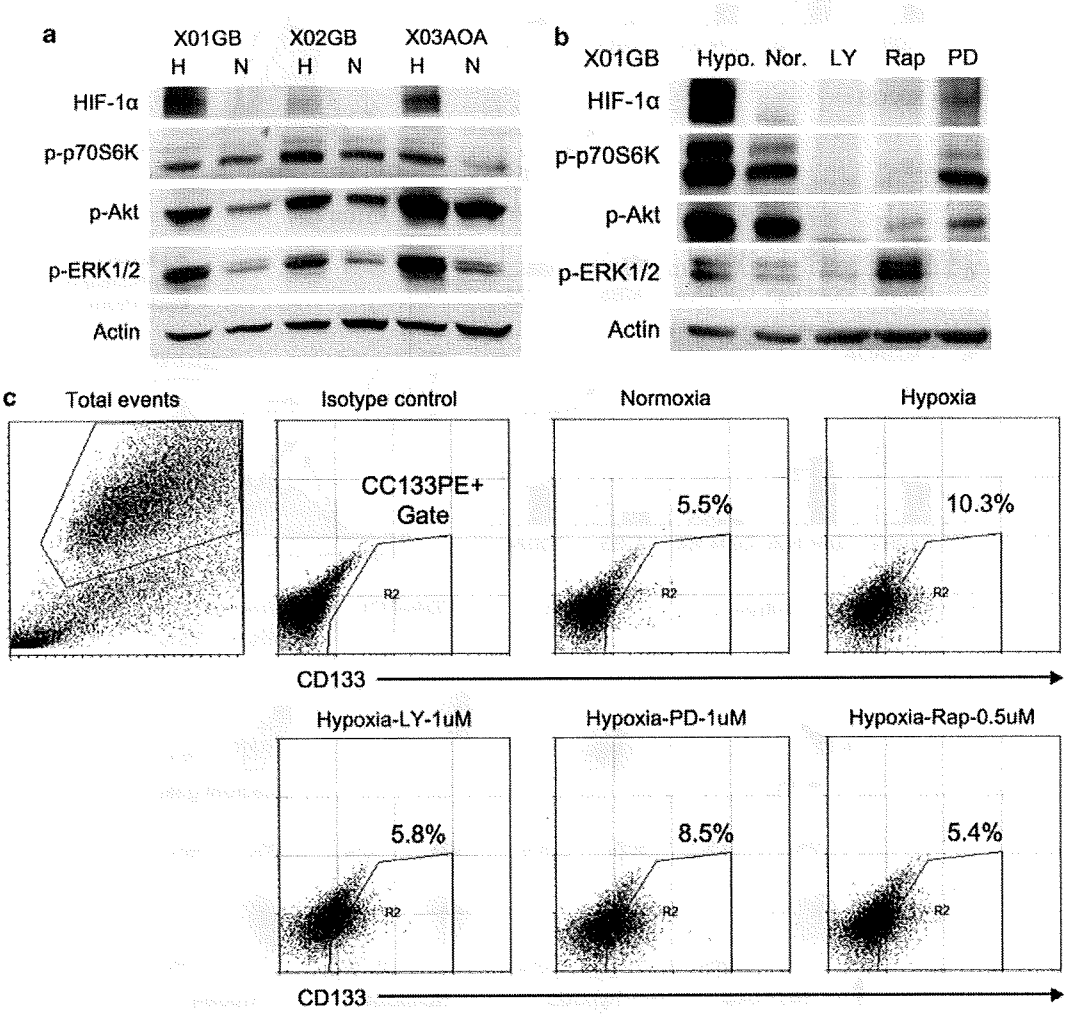

Figure 4 Hypoxic cellular response interacts with growth factor signaling pathway. (**a**) In the absence of the exogenous EGF ligand, hypoxia enhances the phosphorylation of p70S6K, Akt and ERK. (**b**) Hypoxic induction of hypoxia-inducible factor-1α (HIF-1α) is attenuated by growth factor signaling pathway inhibitors. Cancer stem cells (CSCs) were pretreated with LY294002-10 μM (LY), PD98059-20 μM (PD) and rapamycin-5 μM (Rap) for 2 h before 2 h of incubation in a hypoxic environment. Growth factor signaling inhibitors suppress HIF-1α expression under hypoxia. Data are from X01 CSC line representative experiment repeated at least three times. (**c**) Inhibition of the PI3K and ERK pathways independently suppresses the hypoxia-mediated expansion of CD133-positive CSCs. The total number of CD133-positive CSCs at 20% oxygen, 1% oxygen, and with exposure to LY294002 (LY; 1 μM), PD98059 (PD; 1 μM) and Rapamycin (Rap; 0.5 μM) was determined by fluorescence-activated cell sorting dot plot analysis. Data are from X03 CSC line representative experiment repeated at least three times.

(CD184), CD44, A2B5 and CD24 was examined. Propagation at hypoxia led to an increase in the number of cells bearing CXCR4, CD44^{low}, A2B5 and CD24, with a reduction in CD44^{high}-expressing cells (Figures 5a–c). Fluorescence-activated cell sorting dot plot analyses show an overall reduction in the proportion of CD44-positive cells and an increase in the CD133- and CXCR4-positive cells with exposure to hypoxia (Figure 5d). These results show that hypoxia preferentially expands the CD133/CXCR4/CD44^{low}/A2B5/CD24-positive sub-population of CSCs.

Hypoxia inhibits CSC differentiation

To determine the role of hypoxia in the maintenance of the undifferentiated state, we compared the phenotype of CSCs propagated at varying oxygen tensions. Cells plated at a density of 1000/cm^2 under different

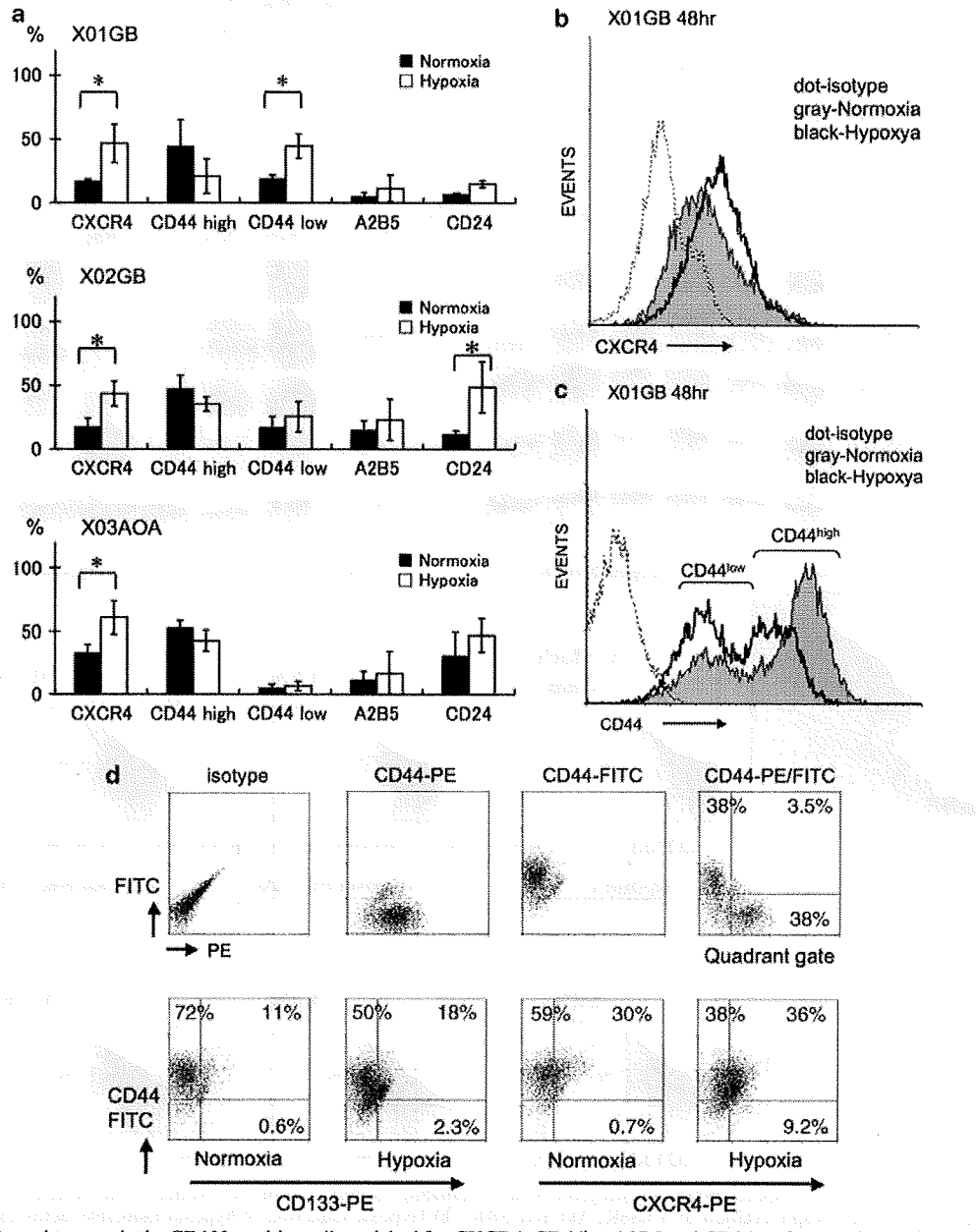

Figure 5 Hypoxia expands the CD133-positive cells enriched for CXCR4, CD44^{low}, A2B5 and CD24 surface markers. (**a**) Cancer stem cell (CSC) lines show a statistically significant expansion of CXCR4 under hypoxia. The X01 lines showed significant expansion of CD44^{low}, and X02GB showed a statistically significant expansion of CD24. (**b**) Representative fluorescence-activated cell sorting (FACS) histogram for X02GB CSC shows expansion of CXCR4-positive cells in hypoxia. (**c**) Representative FACS histogram for X01GB CSC shows expansion of CD44^{low} in hypoxia. (**d**) Representative FACS dot plot analysis for X03AOA CSC shows that hypoxia results in increase in the number of CXCR4 and CD133. Cells exposed to a hypoxic environment for 48 h were fixed and analysed by FACS. Data are from representative experiments repeated at least three times.

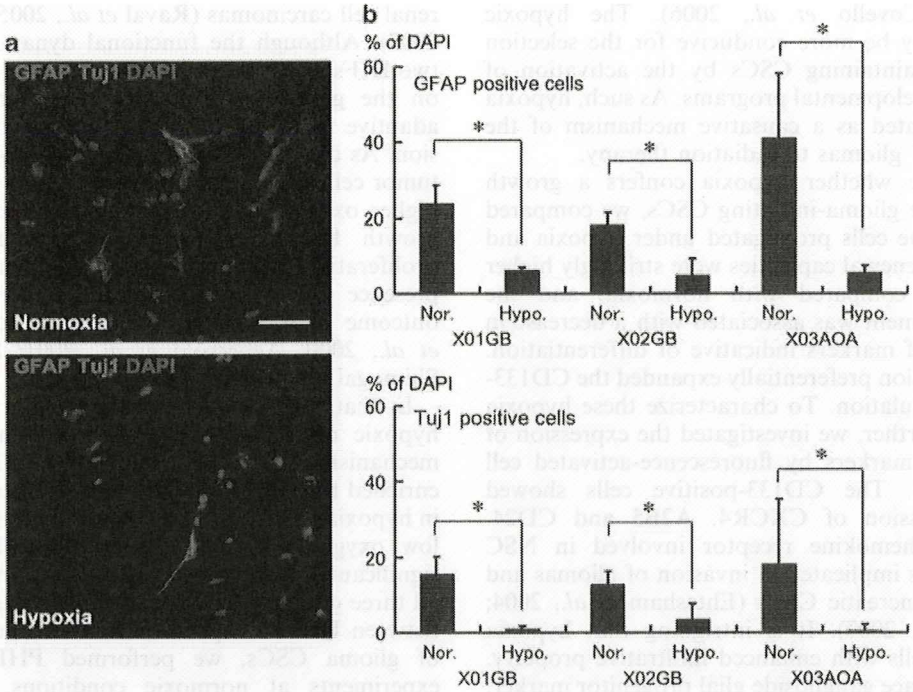

Figure 6 Hypoxia maintains undifferentiated cancer stem cells (CSCs). (**a**) Normoxia induces differentiation of glioma CSCs. Representative colonies were stained with glial fibrillary acidic protein (GFAP) (astrocytic marker) and Tuj1 (neuronal marker) under 20 and 1% oxygen tensions with a medium supplemented with 10% serum. Bar = 50 μm. (**b**) The number of cells expressing lineage-restricted markers was strikingly reduced in cells propagated at hypoxia compared with normoxia. The results shown in the graph are means ± s.d. from three experiments. $^*P<0.05$.

conditions were analysed by indirect immunofluorescence microscopy using two lineage-restricted markers: glial fibrillary acidic protein (astrocytic) and Tuj-1 (neuronal). A greater number of cells were present (almost two-fold) at hypoxia than at normoxia. In addition, the number of cells expressing the differentiation markers was significantly reduced in cells propagated at hypoxia compared with CSCs cultured at normoxia (Figures 6a–b). These data indicate that hypoxia promotes proliferation of CSCs and maintains their undifferentiated phenotype.

Discussion

Determining the growth-promoting mechanisms of the tumor microenvironment will enhance our understanding of cancer biology and may identify new therapeutic approaches. In this study, we investigated the role of hypoxia on glioma CSC maintenance and growth, and sought to identify a potential mechanism. We found that hypoxia confers a growth advantage to CSCs by promoting self-renewal of the CD133-positive cells through an HIF-1α-dependent mechanism and further contributes to tumor pathogenesis by maintaining the CSCs in the undifferentiated state.

Growth of CSCs in hypoxia

Neural stem cells are regulated by extracellular microenvironmental cues to maintain the self-renewal capacity and the undifferentiated state (Wurmser *et al.*, 2004). Recent studies implicate oxygen tension as a key regulator of the NSC metabolic state, survival and fate (Gustafsson *et al.*, 2005; Chen *et al.*, 2007). That tumors are hypoxic is well known, but the reasons are less clear. Most solid tumors, including gliomas, are well vascularized and their growth depends on vascular formation (Louis *et al.*, 2007). This is the fundamental principle behind the antiangiogenesis strategy in cancer therapy (Folkman, 1971). Tumor development is characterized by an initial phase of rapid expansion, followed by a period of slowed growth as the proliferating tumor cells outstrip the local supply of oxygen and nutrients (Louis *et al.*, 2007). Although many tumor cells respond to this metabolic stress through induction of the apoptotic mechanism, some cells may be able to cope with this stress through alterations in cellular metabolism (Li *et al.*, 2004). These cells may subsequently stimulate neovascularization and contribute to further growth of the tumor (Zagzag *et al.*, 2000; Bao *et al.*, 2006b; Oka *et al.*, 2009). Hypoxia also contributes to tumor growth by changing the metabolic state of the cells, resulting in the production of macromolecules needed for cellular proliferation (DeBerardinis *et al.*, 2008). In the hypoxic environment, tumor cells rely more on glycolysis for energy production without complete oxidation of the intermediates. Another tumorigenic property of hypoxia is the activation of specific pathways and transcription factors that control stem cells, such as Notch and Oct4 (Gustafsson

et al., 2005; Covello *et al.*, 2006). The hypoxic environment may be more conducive for the selection of the tumor-maintaining CSCs by the activation of specific early developmental programs. As such, hypoxia has been implicated as a causative mechanism of the poor response of gliomas to radiation therapy.

To investigate whether hypoxia confers a growth advantage to the glioma-initiating CSCs, we compared the growth of the cells propagated under hypoxia and normoxia. Self-renewal capacities were strikingly higher under hypoxia compared with normoxia, and the hypoxic environment was associated with a decrease in the expression of markers indicative of differentiation. Low oxygen tension preferentially expanded the CD133-positive sub-population. To characterize these hypoxia response cells further, we investigated the expression of various surface markers by fluorescence-activated cell sorting analysis. The CD133-positive cells showed increased expression of CXCR4, A2B5 and CD24. CXCR4 is a chemokine receptor involved in NSC migration, and is implicated in invasion of gliomas and metastasis of pancreatic CSCs (Ehtesham *et al.*, 2004; Hermann *et al.*, 2007). It is intriguing that hypoxia might expand cells with enhanced infiltrative property. A2B5, a cell surface ganglioside glial progenitor marker, is a putative CSC marker also associated with tumor recapitulation in xenografts (Ogden *et al.*, 2008). Finally, high levels of CD24 expression have been used to identify transit-amplifying cells as well as differentiated neurons, and CD24 is required for the terminal differentiation of neuronal progenitors (Nieoullon *et al.*, 2005; Panchision *et al.*, 2007). Hypoxia confers a growth advantage to the glioma CSCs by amplifying a distinct sub-population of undifferentiated CD133-positive cells enriched for CXCR4, A2B5 and CD24 surface markers.

HIF-1α-mediated mechanism of growth

Both normal and tumor cells respond to a decrease in ambient oxygen tension by increasing the expression of HIF molecules. HIFs, a member of the basic-helix-loop-helix family of transcription factors, are heterodimers of an α- and β-subunit (Wang and Semenza, 1993; Wang *et al.*, 1995). Although the β-subunit is constitutively expressed, the α-subunit is stabilized only at low oxygen tension. At normoxia, the α-subunit undergoes prolyl hydroxylation and is targeted for degradation by the von Hippel–Lindau tumor suppressor protein (Iliopoulos *et al.*, 1996; Semenza, 2003). The hypoxic microenvironment of tumors results in changes in metabolism, angiogenesis and survival of the cells that are orchestrated by HIF-1α, and, depending on tissue specificity, also by HIF-2α (Keith and Simon, 2007). Both HIF-1α and HIF-2α stimulate the expression of genes involved with angiogenesis, whereas the former also activates glycolytic enzyme gene transcription for adenosine triphosphate synthesis in an oxygen-independent manner (Keith and Simon, 2007). Another difference between the two HIFs is that HIF-2α is capable of activating genes encoding transforming growth factor-α and cyclin D1, and enhancing the c-Myc function in renal cell carcinomas (Raval *et al.*, 2005; Gordan *et al.*, 2007). Although the functional dynamics between the two HIFs are likely to be tissue-specific, tumor cells rely on the gene expression programs directed by these adaptive transcription factors for growth and progression. As the tumor tissue is heterogeneous with hypoxic tumor cells in close proximity to tumor cells exposed to higher oxygen tension, the increased secretion of pro-growth factors by the hypoxic cells may induce proliferative activity of the neighboring cells. The presence of HIFs has been associated with poor outcome in a variety of different neoplasms (Birner *et al.*, 2000; Aebersold *et al.*, 2001; Semenza, 2003; Shimogai *et al.*, 2008; Li *et al.*, 2009).

In that HIF stabilization is a major effector of the hypoxic response, we hypothesized an HIF-mediated mechanism for the expansion of CD133-positive cells enriched for CXCR4, A2B5 and CD24 surface markers in hypoxia. HIF-1α was detectable in cells propagated at low oxygen tension and HIF-1α depletion led to a significant reduction in the sphere-forming capacity of all three glioma CSC lines. To further establish the link between HIF-1α expression and enhanced self-renewal of glioma CSCs, we performed PHD2 knockdown experiments at normoxic conditions. Although the depletion of PHD2 led to low-level expression of HIF-1α at normoxia, there was no effect on self-renewal of CSCs as assessed by sphere formation. As the HIF-1α expression level at 1% oxygen is significantly greater than that seen with PHD2 depletion, we speculate that with the CSC lines we have studied, the PHD2 knockdown approach alone may be insufficient in inducing adequate HIF-1α to promote self-renewal activity. Combined depletion of both PHD2 and factor-inhibiting HIF-1 may be necessary to retain sufficient HIF-1α at normoxia.

Interestingly, knockdown of HIF-1α using siRNA showed an incomplete reduction of CD133-positive cells. Even with the complete inactivation of HIF-1α as seen by the immunoblot, a subtle expansion of CD133-positive cells was seen. This suggests the presence of another mechanism for hypoxia-induced CD133-positive CSC expansion distinct from HIF-1α. As earlier work with renal cell carcinoma showed that HIF-2α regulates transforming growth factor-α, cyclin D1 and c-Myc, we considered the possibility that both factors may be contributing to the hypoxia-induced expansion of CD133-positive CSCs (Raval *et al.*, 2005; Gordan *et al.*, 2007). However, we did not detect changes in the level of HIF-2α, in CSCs cultured at different oxygen tensions. Furthermore, HIF-2α depletion studies failed to show changes in the self-renewal capacity of the CSC. Although this does not definitively exclude an HIF-2α response in the glioma CSC lines we have studied, it does illustrate the importance of determining regional tissue tumor-specific mechanisms. Also, it was reported earlier that Notch signaling may be necessary for hypoxia-mediated stem cell maintenance (Gustafsson *et al.*, 2005). Notch1-specific depletion did not decrease the sphere formation capacity of the three CSC lines studied here.